Czech Technical University in Prague
Faculty of Electrical Engineering
Department of Electrical Power Engineering

MODELLING OF SYNCHRONOUS RELUCTANCE MOTOR

by

EMRE ŞAKAR

A master thesis submitted to
the Faculty of Electrical Engineering, Czech Technical University in Prague.

Master degree study programme: Electrical Power Engineering

Prague, June 2019

Supervisor:

Ing. Petr Liškář
Lead Engineer
Vehicle Electrification eMobility
EATON European Innovation Center
Borivojova 2380
252 63 Roztoky
Czech Republic

MASTER‘S THESIS ASSIGNMENT

I. Personal and study details

Student's name: **Sakar Emre** Personal ID number: **472173**

Faculty / Institute: **Faculty of Electrical Engineering**

Department / Institute: **Department of Electrical Power Engineering**

Study program: **Electrical Engineering, Power Engineering and Management**

Branch of study: **Electrical Power Engineering**

II. Master’s thesis details

Master’s thesis title in English:

Modelling of Synchronous Reluctance Motor

Master’s thesis title in Czech:

Modelování synchronního reluktančního motoru

Guidelines:

1. Introduction to the Synchronous Reluctance Motor (SynRM)
2. Mathematical modeling of SynRM
3. Control Methods for SynRM
4. Model-in-the-loop (MIL) setup of a Controller<->Inverter<->SynRM<->Vehicle
5. Simulation Results and Evaluations

Bibliography / sources:

[1] Peyman Niazi, Hamid A. Toliyat, Dal-Ho Cheong, and Jung-Chul Kim: A Low-Cost and Efficient Permanent-Magnet-Assisted Synchronous Reluctance Motor Drive. IEEE Trans. on Industry Applications, vol.43, no.2, pp.542-550, March/April 2007.
[2] Roberto Morales-Caporal, and Mario Pacas: Encoder less Predictive Direct Torque Control for Synchronous Reluctance Machines at Very Low and Zero Speed. IEEE Trans. On Industrial Electronics, vol. 55, no. 12, pp.4408-4416, December 2008.
[3] Silverio Bolognani, Luca Peretti, and Mauro Zigliotto: Online MPTA Control Strategy for DTC Synchronous-Reluctance-Motor Drives. IEEE Trans. on Power Electronics, vol.26, no.1, pp.20-28, January 2011.

Name and workplace of master’s thesis supervisor:

Petr Liškář, EATON

Name and workplace of second master’s thesis supervisor or consultant:

Date of master’s thesis assignment: **28.02.2019** Deadline for master's thesis submission: **24.05.2019**

Assignment valid until: **19.02.2021**

Petr Liškář Supervisor’s signature	Head of department’s signature	prof. Ing. Pavel Ripka, CSc. Dean’s signature

III. Assignment receipt

The student acknowledges that the master’s thesis is an individual work. The student must produce his thesis without the assistance of others, with the exception of provided consultations. Within the master’s thesis, the author must state the names of consultants and include a list of references.

. | Date of assignment receipt | Student’s signature

Decleration

I, Emre ŞAKAR declare that this thesis and the work presented in it titled Modelling of Synchronous Reluctance Motor are my own and has been generated by me as the result of my own original research. I confirm that this work was done wholly or mainly while in candidature for Masters degree in Electrical Power Engineering at Czech Technical University. Where any part of this thesis has previously been submitted for a degree or any other qualification at this University or any other institution, this has been clearly stated. Where I have consulted the published work of others, this is always clearly attributed. Where I have quoted from the work of others, the source is always given. With the exception of such quotations, this thesis is entirely my own work. I have acknowledged all main sources of help. None of this work has been published before submission.

Date:

Signature:

Abstract

Recently, improvement on electric motor control technologies gathers the attention of researchers on synchronous reluctance motor(SynRM) which have been considered as a possible alternative motor drive for high performance applications. The reason that SynRM is acceptted as alternative motor drive is that it combines the benefits of induction motor(IM) and permanent-magnet synchronous motor(PMSM).

Several types of control strategies have been proposed by researchers. Consequently, maximum torque per ampere(MTPA) strategy is indicated as a reasonable control strategy for SynRM. In addition, sensorless vector controlled drive systems for SynRM become progressively attractive for high-performance drive systems.

In this thesis, SynRM is investigated in state space domain and mathematical modelling of SynRM is executed in d-q reference frame. MTPA and sensorless speed control systems are introduced and simulated with the SynRM. Simulations are performed with Matlab/Simulink. Various electrical and mechanical behaviors of the motor are analyzed.

Keywords:

Synchronous Reluctance Motor, Maximum Torque Per Ampere, Sensorless Speed Control, MATLAB/Simulink.

Abstrakt

Současný pokrok na poli řízení elektrických motorů dostává do popředí zájmu synchronně reluktanční motory, které jsou považovány jako alternativní pohon pro aplikace vyžadujících vysokých výkonů. Důvodem zvýšeného zájmu o tento druh pohonu je kombinace výhod indukčního motoru a synchronního motoru s permanentním magnetem.

Nedávné výzkumy navrhují několik možných způsobů řízení tohoto motoru. Metoda maximálního momentu na jednotku proudu (Maximum Torque per Ampere), je považována jako nejlepší možný způsob řízení. Další metodou se značným potenciálem je bezsenzorové vektorové řízení.

Tato diplomová práce zkoumá synchronně reluktanční motory z pohledu stavového prostoru a matematického modelu v d-q osách. Metody MTPA a bezsenzoroveho řízení jsou popsány a následně simulovány na synchronně reluktančních motorech v prostředí Matlab a Simulink, kde je mimo jiné analyzováno elektrické a mechanické chování motoru.

klíčová slova: synchronně reluktanční motor, maximálního momentu na jednotku proudu, bezsenzorové řízení rychlosti, Matlab/Simulink

Acknowledgements

First of all, I would like to express my gratitude to my master thesis supervisor, Mr.Petr Liškář. He has been a constant source of encouragement and insight during my research and helped me with numerous problems and professional advancements.

I would like to thank to Mr.Pavel Kučera, and Mr.Pavel Cejnar for giving me their unflagging support.

I also would like to thank to Prof.Jǐri Lettl for his support and guidance in the begging of my study.

Special thanks go to the staff of the EATON European Innovation Center, who maintained a pleasant and flexible environment for my research.

I would like to express thanks to my colleagues, namely Mr. Emin Tunahan Yazan and Mr. Mustafa Can Uzun, for their valuable comments and support.

Finally, my greatest thanks go to my family members, for their infinite patience and care.

Dedication

To My Family.

Contents

List of Figures

Abbreviations

List of Variables in Equations

ω_s	Synchronous speed
ω_r	Rotor speed
V_{ds}	Direct axis voltage
V_{qs}	Quadrature axis voltage
i_{ds}	Direct axis current
i_{qs}	Quadrature axis current
R_s	Stator resistance
λ_{ds}	Direct axis flux
λ_{qs}	Quadrature axis flux
L_{ds}	Direct axis inductance
L_{qs}	Quadrature axis inductance
L_{ls}	Leakage inductance
L_{md}	Direct axis magnetizing inductance
L_{mq}	Quadrature axis magnetizing inductance
τ_e	Electromagnetic Toruqe
P	Pole pairs number
δ	Stator voltage vector angle
ω_e	Motor speed
I_s	Stator current

V_s	Stator voltage
ϵ	Magneto motive forve angle
γ	Stator current vector angle
τ_l	Load torque
D_f	Damping friction of motor
F_t	Traction force

Miscellaneous Abbreviations

SynRM	Synchronous Reluctance Motor
MTPA	Maximum Torque Per Ampere
AC	Alternating Current
EMF	Electromotive Force
RMF	Rotating Magnetic Field
DC	Direct Current
SP	Salient Pole
ALA	Axially Laminated Antisotropy
TLA	Transversally Laminated Antisotropy
IM	Induction Machine
PMSM	Permanent Magnet Synchronous Motor

Chapter 1

INTRODUCTION

1.1 AC Machines

The usage of AC motors have been on an upward trajectory since the invention of first AC motor, which is also called as Teslas motor, in 1888. Moreover, the usage and the variety of the AC motors are increasing with each passing day. The common reason behind the rise is that AC motors are the largest consumers of electric power. This situation renders AC motors and the related topics as a very attractive field of study and research [1][2].

1.1.1 Definition AC Machines

An AC motor is defined as a motor that is driven by Alternating Current, hence the name. Generally, it consists of two basic parts: stator, which is the external part that is receiving alternate current with its coils; and rotor, which can be defined as the internal part that is producing the rotating magnetic field. According to Adkins and Harley(1975), the basic working principle of an AC motor can be explained as follows: Firstly, in the stator winding, alternating flux is produced by the AC supply. When the alternating flux starts to rotate with synchronous speed, a rotating magnetic field (RMF) is produced on the stator. Due to Faradays law of electromagnetic induction, the relative speed between the stator and the rotor results in an induced electromotive force (EMF). Afterwards, this electromotive force will produce an alternating flux around the rotor. According to Lenzs law, the rotor flux will try to catch up to the stator rotating magnetic field. As a result, the rotor rotates in accordance to the direction of the stator's rotating magnetic field, in order to minimize

relative velocity. In other words, the rotor will try to reach the synchronous speed. [3]

1.1.2 Types of AC Machines

Depending on the different applications, there is a variety of AC machines. Although they can be classified in several types, the general classification for AC machines can be listed as synchronous and asynchronous machines. A synchronous machine is an electrical machine whose rotating speed is proportional to the frequency of the alternating current supply and independent of the load. In synchronous machines, rotor speed and speed of stator RMF are equal to each other. These kinds of machines are generally used in power stations, manufacturing industries. On the other hand, asynchronous motors are AC motors designed such that the rotor movement is not synchronized with the moving stator field. The rotating magnetic field induces a current in the rotor windings and it generates a force drawing the rotor towards to stator.

In asynchronous machines, when the rotor's phase is different from the stator's phase, a torque can be generated.If the rotor were to become aligned with the stator field the torque would disappear thus causing the rotor to pause. This situation is creates a lag which is called as slip. Asynchronous machines are mostly used in pumps, fans, compressors and lifts. Moreover, there are several more differences between synchronous and asynchronous machines. For instance, synchronous machines do not have a slip component whereas asynchronous machines have a slip component. Therefore, the value of slip is not equal to zero in asynchronous machines.

$$Slip = (\frac{\omega_s - \omega_{rotor}}{\omega_s}) * 100 \tag{1.1}$$

Synchronous machines start as an induction machine and as the motor approaches synchronous speed, excitation on the rotor is turned on by applying DC power. The rotor is locked in and synchronized with the stator field. Asynchronous machines do not require any additional starting source. By changing excitation, the power factor of the synchronous machines can be adjusted accordingly as lagging, leading or unity; whereas asynchronous machines are only capable of running at a lagging power factor.[14]

In addition to the aforementioned types, there are also different kinds of classifications

for AC motors such as single-three phase motors, constant-adjustable speed motors and varied structure motors.

1.1.3 Type of Drives of AC Machines

In order to control AC motors, a variety of methods have been developed since the invention of the first induction machine. Nowadays, AC motors are usually being controlled by AC controllers, which can also be referred to as variable frequency drives or adjustable speed drives. These controllers consist of rectifiers, inverters and a DC link between them. To start with, AC input is converted to DC before being stored in the DC link by the inverters. Then, by controlling the inverter, it is possible to obtain a frequency controlled AC output. Controlling the frequency of the output allows adjusting the speed of motor in accordance with the motors load. Furthermore, for different applications of adjusting frequency, there are 3 general types of drives are used in todays electric industry. These types are called current source inverter, voltage source inverter and direct frequency converter such as cycloconverter. These inverters and converters commonly include semiconductor switches such as MOSFET and IGBT which are generally controlled with pulse width modulation (PWM).[4][5][6]

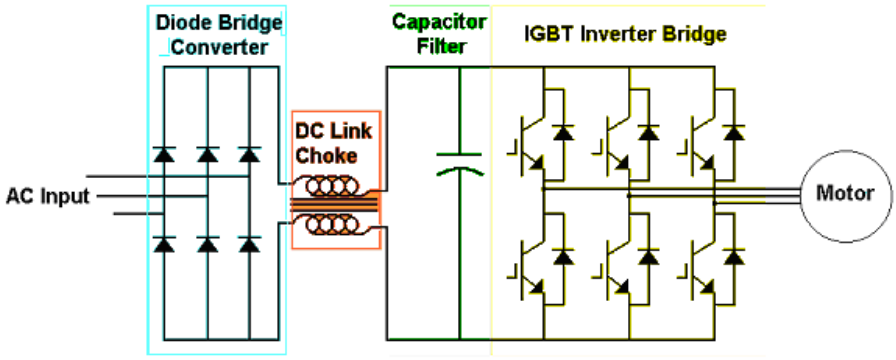

Figure 1.1: An Example of Variable Frequency Drives [27]

1.2 The Synchronous Reluctance Motor (SynRM)

During the 1920s, after realizing that using permanent magnets in the motors increase their efficiency and performance, the synchronous reluctance motor was invented. However, it was not able to be used in industrial applications because of its inadequate efficiency and torque characteristics which hold a lot of torque ripple in low speeds. Today, synchronous reluctance motors are more widely used thanks to the improvements within the power electronics industry [12].

Figure 1.2: Synchronous Reluctance Motor (SynRM) [8]

1.2.1 Definition SynRM

The concepts of magnetic reluctance and rotating magneto motive force allow the operation of synchronous reluctance motors. From the basics of magnetic field theory, it is known that when a magnetic field is applied to an asymmetric object with an angle difference (δ)

between its d-axis and q-axis, it starts to produce torque as shown in Fig2.

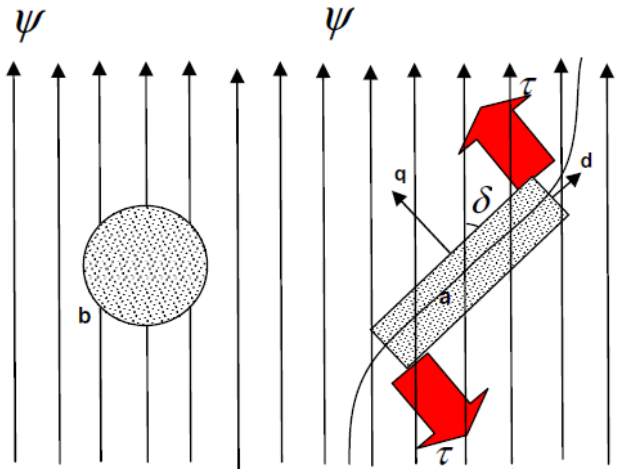

Figure 1.3: An Object with Asymmetric Geometry (a) and Isotropic Geometry (b) In a Magnetic Field Ψ and Torque Production Mechanism [28].

Synchronous reluctance motor (SynRM) is a three-phase brushless AC electric motor with a magnetically asymmetric rotor structure that consists of a conventional DC permanent magnet machine, a permanent magnet synchronous machine and the cage of an induction machine[8]. Thereby, the stator of a SynRM is identical to the stator of an induction machine. Inner surface of the stator is also cylindrical, which allows it to have several advantages of the AC motors while also eliminating some disadvantages [7]. As Mr. Matyska stated, SynRM combines the benefits of the induction motors and the permanent magnet motors, such as robustness of an induction motor and the size, efficiency and synchronous speed operation benefits of permanent magnet motors. Moreover, SynRM can be controlled by sensorless control due to high saliency of rotor [9]. However, construction of the rotor is more complicated than that of the stator because there is no excitation winding in the rotor. Hence, the rotor is constructed with salient reluctance poles.

The portions of the rotor poles are configured with a specific distance that is determined to be as short as possible between the permanent magnets. On the other side, the permanent magnets are typically preferred to be designed as large as possible in order to use flux more efficiently and to minimize the flux leakages [10]. Primarily, SynRM has three different types of asymmetric structures as illustrated in Figure 1.4.

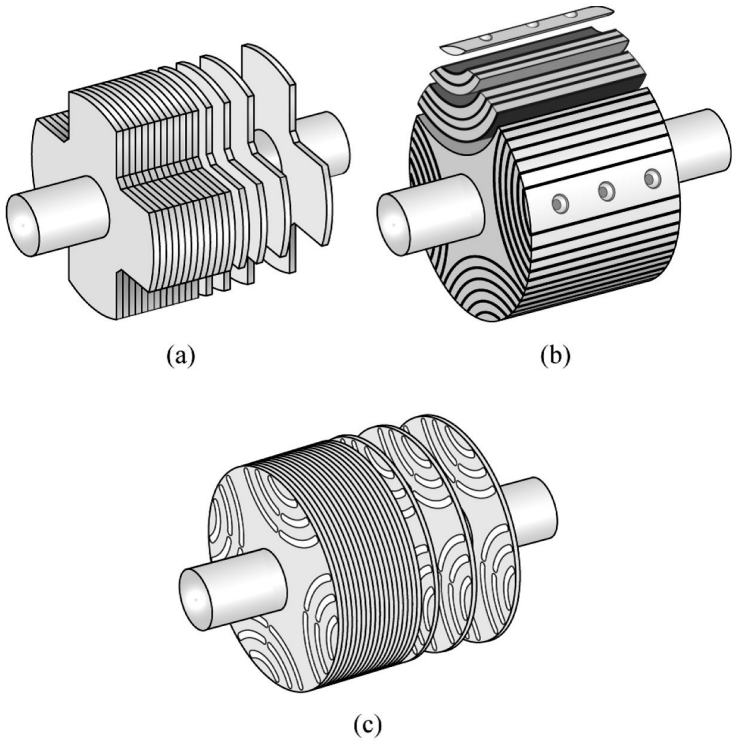

Figure 1.4: Possible Rotor Designs for a SynRM: (a) Simple Salient Pole (SP) Rotor, (b) Axially Laminated Anisotropy (ALA) Rotor, (c) Transversally Laminated Asymmetric (TLA) Rotor [28]

In the first rotor type, the salient pole rotor or conventional rotor arrangement, the construction is carried out by eliminating some of the iron metal from each rotor. It was the starting point of SynRM development, so it is also called a first generation SynRM. However, due to its low saliency ratio and consequently low performance, their use cases were limited to only a few applications.

In the axially laminated rotor, which is the second type of rotor, the laminations are designed smoothly to intertwine. There are also insulation layers between the iron laminations, which are built with electrically and magnetically passive materials. Moreover, complete batches are connected into pole holders through the shaft as shown Figure1.4 (b).

Based on its design with the starting cage, the performance expectations were high from

the axially laminated SynRM, but saliency ratio was not able to be controlled completely until the end of the 1980s. After the 1980s, an axially laminated SynRM without a cage was built and it produced an efficient performance by increasing its saliency ratio. As a result, SynRM was begun considering as an alternative for electric motors. [11]

The next generation of rotor type is called transversally laminated rotor, as illustrated in figure 1.4 (c). Its laminations are constructed in the traditional way, same as cylindrical permanent magnet rotors, but it is shaped in thin ribs for flux paths. Then, numbers of rotor segments are connected to each other with thin ribs. As a result, constructions of the laminations are easier and cheaper when compared to the previous models. However, it has less of a power factor and produced torque compared to the axially laminated SynRM because transverse laminations cause more leakage than axial laminations. [13]

The latest improved rotor type is called a permanent magnet assisted SynRM. Actually, it is a type of axially laminated and transversally laminated rotor with the addition of some permanent magnets, which increases the saliency ratio in the rotor core as shown in Figure 1.5. Figure1.5.

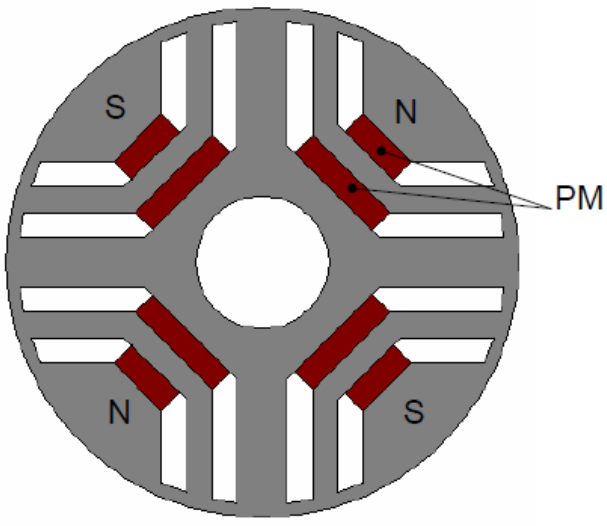

Figure 1.5: Four-Pole Transversally-Laminated Permanent Magnet (PM) Assisted Rotor[26]

1.2.2 Working Principle of SynRM

The stator of the SynRM is designed with two different windings, which are called main windings and auxiliary windings, because the main winding is not able to produce a rotating magnetic field by itself. In order to create a rotating magnetic field, it is required to have a certain phase angle between the main and auxiliary windings. Therefore, SynRM has additional, auxiliary windings apart from the other motors. The difference at the phase angles result in some difference in the corresponding fluxes. Such a difference creates the rotating magnetic field at a constant speed which is equal to the synchronous speed.

For starting the rotor, it is essential that the rotor has aluminum or copper bars, so that it can fall under the influence of the rotating magnetic field in a comparable level to that of the induction motor with squirrel cage rotor. Once the rotor is under the influence of the rotating magnetic field, it aligns itself according to the minimum reluctance paths and then it fastens itself to the rotating magnetic field. Afterwards, the rotor rotates with a constant speed which equals to the synchronous speed. While the rotor starts to rotate with synchronous speed, a considerably high torque is able to come to existence and such phenomenon is called reluctance torque. As a result, the SynRM works as a synchronous motor.

1.2.3 Controlling Methods For SynRM

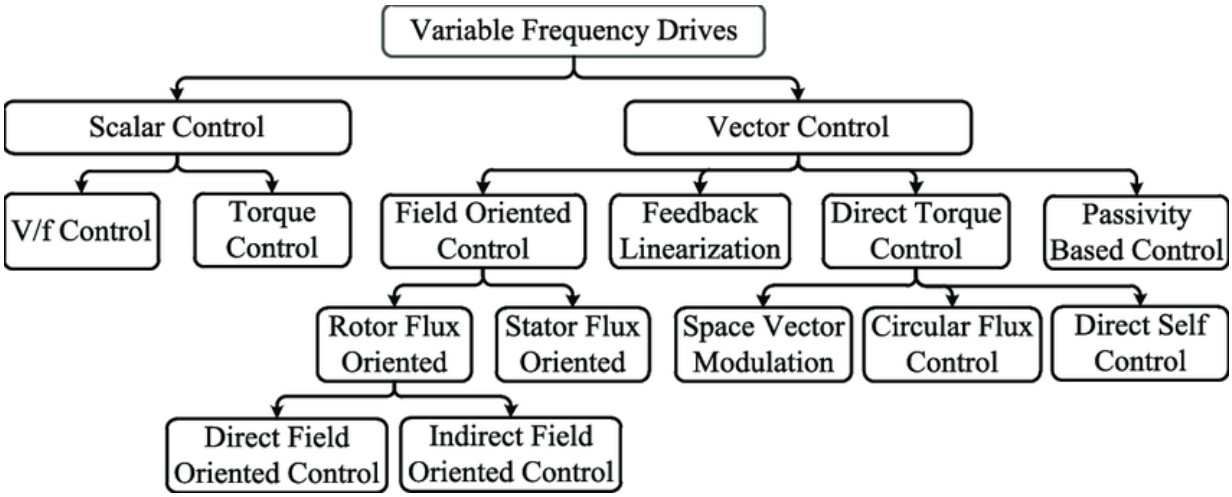

Figure 1.6: Varieties of Variable Synchronous Drives [29]

For many years synchronous motors have been widely used for industrial purposes. And as a result, the control of synchronous motors is one of the most vital topics in the electric motor industry. During the development process of electric motor drives, different kinds of variable frequency drives were employed in order to be able to be driven at various speeds. Although the main circuit schematics idea is similar in most of the variable frequency drives, which is shown in figure 1.6, the control methods can be separated into two main categories. These categories are scalar and vector control, depending of their controlling purpose [5].

In order to control only magnitudes of the voltage and the current, scalar control algorithms are employed. On the other hand, vector control algorithms allow controlling not only magnitudes of voltage and current but also the phase angles.

In the 1960s, the vector control methods were not improved enough to utilize SynRM. As a result, researchers were trying to drive the SynRM with conventional V/f and torque control algorithms, where the relationship between the voltage or the current and the frequency are kept constant through the motors speed range. However, it was not enough to enhance the drive performance and stabilize the synchronous operation down to low speeds. After the improvement of rotor designs and vector control algorithms, where control of both the magnitude and the angle of the flux are possible in order to achieve higher dynamic performance of the drive system compared to what the scalar control can provide, studies were accelerated to make SynRM a more competitive alternative compared to the other brushless AC motors.

Nowadays, modern control methods consist of model based and parameter dependent algorithms. Varieties of direct torque control and field oriented control are widely employed to drive SynRMs. In this paper, Maximum Torque per Ampere (MTPA) technique will be investigated and a speed controlled SynRM will be simulated.

1.3 Organization of Thesis

In order to guide the stated research objectives, this master thesis is outlined as following:

Chapter one introduces the background knowledge about AC motors and particularly synchronous reluctance motors. In this chapter, description and types of AC motors are provided. In particular, definition and principles of SynRM is explained. Moreover, basics of control strategies of AC motors are also provided.

Chapter two provides detailed information on mathematical perspectives of the SynRM. Equivalent circuit of SynRM is represented in state space domain and accordingly d-q model of the SynRM is derived from this circuit. Also, steady state model of SynRM and its phasor equations are shown in this chapter. In addition, this chapter includes torque expressions and calculations for maximum power factor.

Chapter three emphasizes the importance of control of SynRM and explains two types of control strategies based on speed control and torque control. For the speed control, sensorless speed control method is investigated and constructed simulation block is illustrated. For the torque control, Maximum Torque per Ampere (MTPA) strategy is analyzed. The block diagram of the control strategy is explained.

Chapter four studies the simulation block diagrams and their results. Simulations are carried out in MATLAB/Simulink. Simulink and Simscape libraries are employed. Firstly, SynRM is simulated in no load condition with sensorless speed controller. Then, a load torque applied on SynRM and the effects of load torque on motors electrical and mechanical behaviors are observed. Furthermore, MTPA strategy is practiced on the SynRM and results are captured. Since only difference is the control strategy in the simulations, the differences between the MTPA and sensorless speed control are observed. In addition, traction effort curve is plotted to investigate loadability of the motor.

Chapter five supplies a brief summary of this thesis and highlights the key points of every chapter. Afterwards, it expresses the objective of thesis is fulfilled.

1.4 Research Objectives

The purpose of this thesis is to investigate electrical and mechanical behaviors of synchronous reluctance motors. This has been accomplished by carrying out a literature review over existing control strategies and designing the SynRM by using the mathematical modelling of it in the simulation tool Simulink.

The first objective to fulfill the aim of this investigation is to model the SynRM and control methods with mathematical perspective in Simulink. Then, complete Simulink models will be designed by creating a closed loop system for speed control and maximum torque per ampere method connected with SynRM.

As a result, after specifying all the parameters, the simulation results with respect to both control method will be able to be observed. Therefore, the second objective of this thesis is to compare the results that are obtained from the Simulink and to provide a comparison between specified parameters for both control method. This comparison will constitute a substantial collection of background information for further studies on synchronous reluctance motors.

Chapter 2

MATHEMATICAL MODELLING OF SYNCHRONOUS RELUCTANCE MOTOR

2.1 d-q State Phasor Model of SynRM

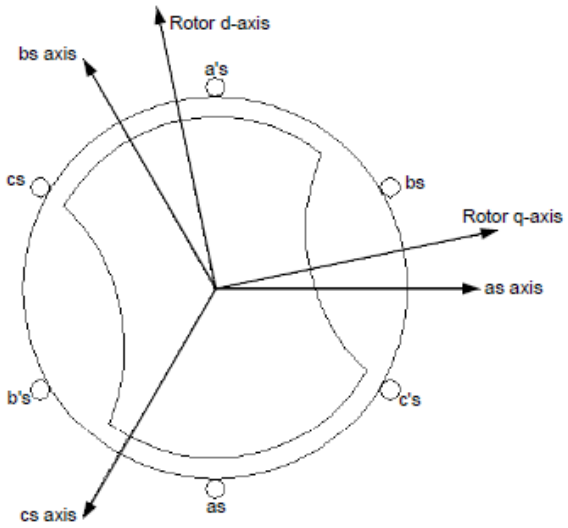

Figure 2.1: Two pole Synchronous Reluctance Motor (SynRM) with d-q Axis [30]

In this chapter, a basic 2 pole synchronous reluctance machine which is shown in figure 2.1 will be investigated in order to observe mathematical equations of the machine. The indicated SynRM has 3-phase stator with the salient pole rotor. The stator windings are constructed as identical windings which has 120 degree angular difference between each other with N_s equivalent turns and resistance of R_s.

Since the stator winding of SynRM is sinusoidally distributed, flux harmonics in the air gap contribute only to an additional term in the stator leakage inductance [15].Therefore, the equations for presenting the behavior of the SynRM can be derived from conventional equations of a conventional wound field synchronous machine.

As stated in previous chapter synchronous reluctance motor does not have an excitation winding and also it does not require a rotor cage because SynRM can be started to operate synchronously from zero speed by using efficient inverter control [14]. Due to absence of excitation winding and rotor cage, it is possible to eliminate the field winding and damper winding equations from the Parks equations. Then, the d-q equations for a synchronous reluctance machine, which is shown in equation 2-1 and 2-2, can be obtained. Also, the equivalent circuit of SynRM in space phasor can be constructed with d-q axis as shown in figure 2.2.

$$V_{ds} = R_s.i_{ds} + \frac{d\lambda_{ds}}{dt} - \omega_r.\lambda_{qs} \tag{2.1}$$

$$V_{qs} = R_s.i_{qs} + \frac{d\lambda_{qs}}{dt} + \omega_r.\lambda_{ds} \tag{2.2}$$

Where;

$$\lambda_{ds} = L_{ls}.i_{ds} + L_{md}.i_{ds} = L_{ds}.i_{ds} \tag{2.3}$$

$$\lambda_{qs} = L_{ls}.i_{qs} + L_{mq}.i_{qs} = L_{qs}.i_{qs} \tag{2.4}$$

And L_{ls}, L_{md} and L_{mq} are the stator leakage inductances which are direct axis magnetizing inductance (L_{md}) and quadrature axis magnetizing inductance (L_{mq}). R_s is representing the quantity of the stator resistance per phase.

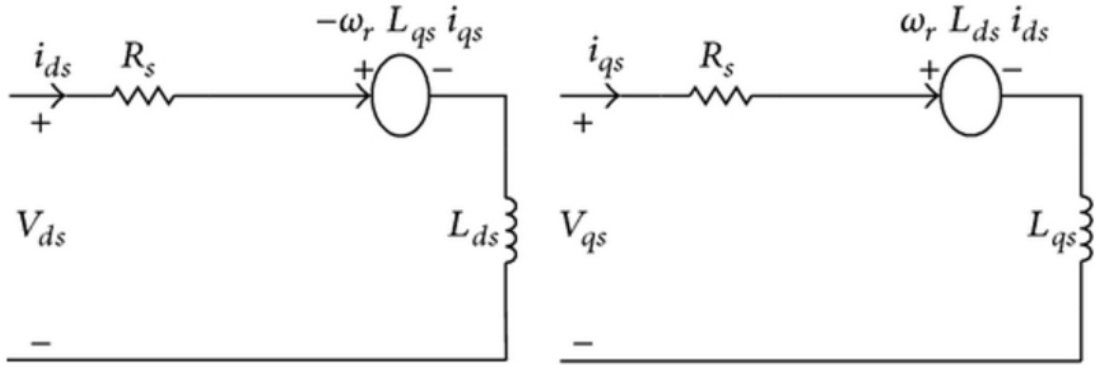

Figure 2.2: d-q Axis Model Equivalent Circuit of Synchronous Reluctance Machine [31]

In terms of the d-q variables, the electromagnetic torque can be obtained as follows,

$$\tau_e = \frac{3}{2}.\frac{P}{2}.(\lambda_{ds}.i_{qs} - \lambda_{qs}.i_{ds}) \tag{2.5}$$

Where P is the number of poles. As equation 2-3 and 2-4 stated the λ_{ds} and λ_{qs} expressions, it is possible to rewrite the electromagnetic torque equation (2-5) in terms of d-q inductances.

$$\tau_e = \frac{3}{2}.\frac{P}{2}.(L_{ds}.i_{qs}.i_{ds} - L_{qs}.i_{ds}.i_{qs}) \tag{2.6}$$

$$\tau_e = \frac{3}{2}.\frac{P}{2}.(L_{ds} - L_{qs}).i_{qs}.i_{ds} \tag{2.7}$$

According to equation 2-7, the inductance differences between d and q axis has an influence on electromagnetic torque. When this difference increases, the electromagnetic torque also rises.

2.2 Steady State Model of SynRM

This d-q model of SynRM allows expressing the behavior of the stator and rotor currents in a reference frame that is rotating with the rotor of the machine. When the SynRM has balanced three phase voltages on it as a source, voltages in d-q axis reach a constant amplitude rotating vector in the d-q plane. By having same angular velocity of the rotating voltage vector with rotors angular velocity, the steady state characteristics can be achieved at the rotor reference frame. In this case, angular relationship between the stator voltage vector and the d-q axis can be described as shown in figure 2.3.

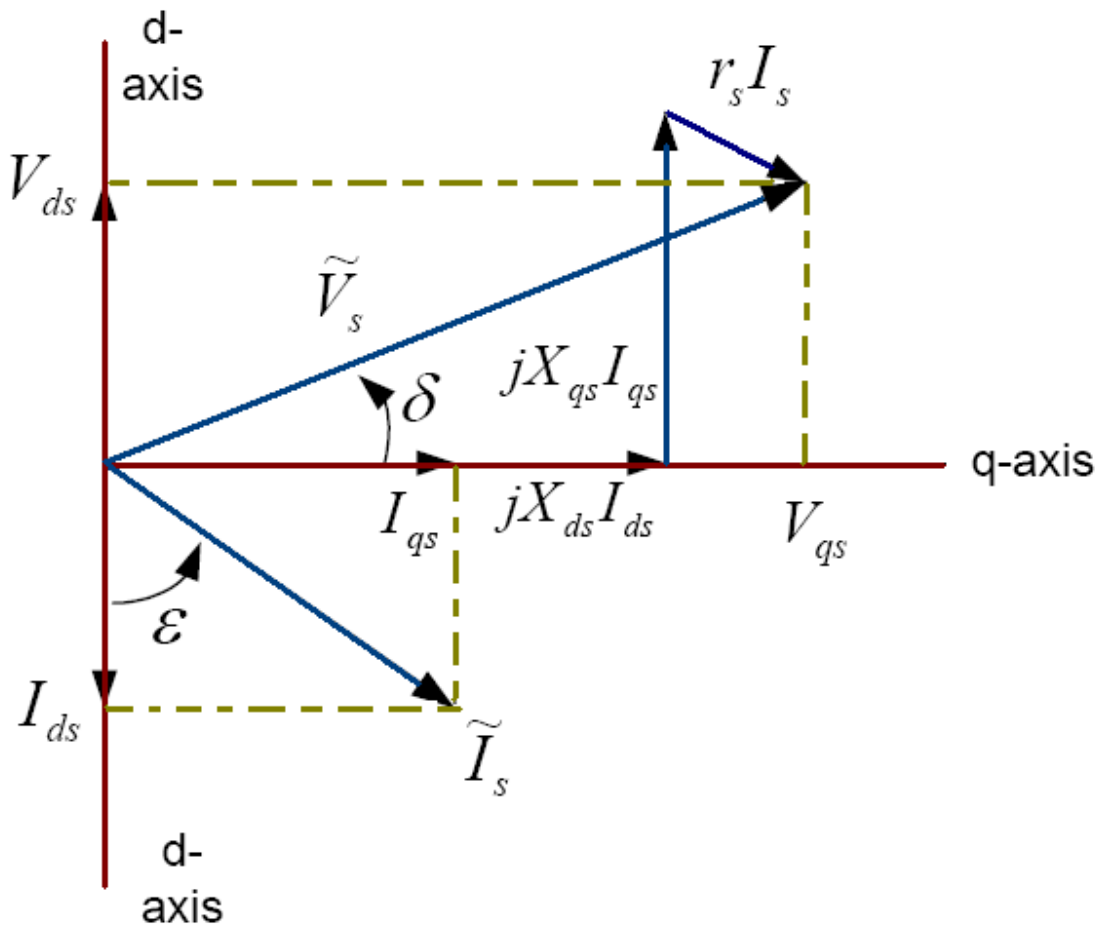

Figure 2.3: Phasor Diagram of Synchronous Reluctance Machine [32]

From the phasor diagram voltages in d-q axis can be derived as follows,

$$V_{ds} = -V_S.sin\delta \tag{2.8}$$

$$V_{qs} = V_S.cos\delta \tag{2.9}$$

The voltage equations for d-q axis which are shown in equation 2-1 and 2-2 become constant in steady state case, so that d/dt terms can be omitted. Consequently, current equations for d-q axis can be derived in terms of steady state voltages as follows,

$$i_{ds} = \frac{\omega_e.L_{qs}.V_{qs} + R_s.V_{ds}}{R_s^2 + \omega_e^2.L_{qs}.L_{ds}} \tag{2.10}$$

$$i_{qs} = \frac{-\omega_e.L_{ds}.V_{ds} + R_s.V_{qs}}{R_s^2 + \omega_e^2.L_{qs}.L_{ds}} \tag{2.11}$$

If stator resistance is eligible, then current equations will be rewrite approximately as,

$$i_{ds} = \frac{V_{qs}}{\omega_e.L_{ds}} \tag{2.12}$$

$$i_{qs} = \frac{-V_{ds}}{\omega_e.L_{qs}} \tag{2.13}$$

2.3 Phasor Equations of SynRM

From the phasor domain perspective, it is possible to drive single phasor equation for steady state case by multiplying the equation 2-1 by j and adding it to the equation 2-2 as shown in below.

$$V_{qs} - j.V_{ds} = R_s.(i_{qs} - j.i_{ds}) + \omega_e(\lambda_{ds} + j.\lambda_{qs}) \tag{2.14}$$

Then, by substituting the equation 2-3 and 2-4 into 2-14,

$$V_{qs} - j.V_{ds} = R_s.(i_{qs} - j.i_{ds}) + \omega_e(L_{ds}.i_{ds} + j.L_{qs}.i_{qs}) \tag{2.15}$$

Equation 2-15 can be manipulated to form of:

$$V_{qs} - j.V_{ds} = R_s.(i_{qs} - j.i_{ds}) + j.\omega_e L_{ds}.(-j.i_{ds}) + j.L_{qs}.i_{qs} \tag{2.16}$$

After the equation 2-16 is derived, voltage equation can be written in phasor notation as follows.

$$\vec{V} = R_s.\vec{I_s} + j.X_{ds}.\vec{I_{ds}} + j.X_{qs}.\vec{I_{qs}} \tag{2.17}$$

Also, the phasor diagram for the equation 2-17 is presented in figure 2.3.

2.4 Torque Expression for Constant Volt per Hertz and Constant Current Operation

Electromagnetic torque equation (2-7) can be analyzed in terms of voltage by substituting equations 2-10 and 2-11.

$$\tau_e = \frac{3}{2}.\frac{P}{2}.(L_{ds} - L_{qs}).\frac{\omega_e.L_{qs}.V_{qs} + R_s.V_{ds}}{R_s^2 + \omega_e^2.L_{qs}.L_{ds}}.\frac{-\omega_e.L_{ds}.V_{ds} + R_s.V_{qs}}{R_s^2 + \omega_e^2.L_{qs}.L_{ds}} \tag{2.18}$$

In the equation 2-18, stator resistance can be neglected approximately by excepting close to zero frequencies. Then, it is reduced to:

$$\tau_e = \frac{3}{2}.\frac{P}{2}.\frac{(L_{ds} - L_{qs})}{(L_{ds}.L_{qs})}(\frac{V_{ds}}{\omega_e}) \tag{2.19}$$

By using the equations 2-8 and 2-9, torque angle (δ) is adapted to torque equation as shown below.

$$\tau_e = \frac{3}{2}.\frac{P}{2}.\frac{(L_{ds} - L_{qs})}{(L_{ds}.L_{qs})^2}\frac{sin2\delta}{2} \tag{2.20}$$

As a result, the electromagnetic torque of SynRM changes with square of volt per hertz and sinus of twice of the torque angle. When the voltage is constant, maximum torque can be achieved in maximum value of the sine of torque angle which is 45 degree. Hence, the maximum torque for a fixed volt per hertz is:

$$\tau_e = \frac{3}{4}.\frac{P}{2}.\frac{(L_{ds} - L_{qs})}{(L_{ds}.L_{qs})^2}(\frac{V_s}{\omega_e})^2 \tag{2.21}$$

In addition, the electromagnetic torque equation can also be derived in terms of stator current from the phasor diagram of synchronous reluctance machine. From figure 2.3, d-q axis currents can be written as;

$$i_{ds} = I_S.cos\epsilon \tag{2.22}$$

$$i_{qs} = I_S.sin\epsilon \tag{2.23}$$

Where ϵ is the magneto motive force angle. Consequently, if the equations 2-22 and 2-23 are substituted into 2-7, electromagnetic torque is expressed in terms of stator current as follows.

$$\tau_e = \frac{3}{2}.\frac{P}{2}.(L_{ds} - L_{qs}).I_S^2.\frac{sin2\epsilon}{2} \tag{2.24}$$

2.5 Maximum Power Factor

One of the biggest disadvantages of synchronous reluctance motor is low power factor since it increases the size of the motor drive, so that reaching maximum power factor is a vital

issue for SynRM [16]. According to phasor diagram in figure 2.3, power factor of SynRM, $cos\phi$, can be written as the ratio of the projection of the voltage vector on the current vector divided by the amplitude of voltage vector as shown in equation 2-25.

$$cos\phi = \frac{V_{qs}.sin\epsilon - V_{ds}.cos\epsilon}{\sqrt{(V_{qs}^2 + V_{ds}^2)}} \tag{2.25}$$

When Vds and Vqs expression from equations 2-12 and 2-13 are substituted into power factor equation by neglecting stator resistance, 2-25 can be written as

$$cos\phi = \frac{\omega_e.L_{ds}.i_{ds}.sin\epsilon - \omega_e.L_{qs}.i_{qs}.cos\epsilon}{\sqrt{(\omega_e.L_{ds}.i_{ds})^2 + (\omega_e.L_{qs}.i_{qs})^2}} \tag{2.26}$$

By using 2-22 and 2-23:

$$cos\phi = \frac{\omega_e.L_{ds}.i_S.cos\epsilon.sin\epsilon - \omega_e.L_{qs}.i_S.sin\epsilon.cos\epsilon}{\sqrt{(\omega_e.L_{ds}.i_S.cos\epsilon)^2 + (\omega_e.L_{qs}.i_S.sin\epsilon)^2}} \tag{2.27}$$

After some reduction:

$$cos\phi = \frac{(L_{ds} - L_{qs}).sin\epsilon.cos\epsilon}{\sqrt{((L_{ds}.cos\epsilon)^2 + (L_{qs}.sin\epsilon)^2)}} \tag{2.28}$$

Then, it is possible to substitute saliency ratio, k= L_{ds}/L_{qs} the equation 2-28 as follows.

$$cos\phi = \frac{k-1}{\sqrt{k^2.\frac{1}{sin^2\epsilon}\frac{1}{cos^2\epsilon}}} \tag{2.29}$$

From the equation 2-29, power factor can be calculated with any saliency ratio, k and magneto motive force angle, ϵ. For the maximum power factor, the magneto motive force

angle can be determined by using equation 2-29. In order to make calculations simpler, sine function can be substitute with an unknown such as $a = sin^2\epsilon$.

$$cos\phi = \frac{k-1}{\sqrt{k^2.\frac{1}{a}\frac{1}{1-a}}} \tag{2.30}$$

For finding maximum value of power factor, $cos\phi$(a) has to be differentiated and solved in terms of a by equalizing to 0.

$$\frac{dcos\phi(a)}{da} = \frac{k-1}{(k^2.\frac{1}{a}\frac{1}{1-a})^{\frac{-3}{2}}}.(\frac{-k^2}{a^2} + \frac{1}{(1-x)^2}) \tag{2.31}$$

After solving the equation 2-31:

$$a = k.(1-a) = k.(1-sin^2\epsilon) = k.cos^2\epsilon \tag{2.32}$$

$$tan\epsilon = \sqrt{k} \tag{2.33}$$

Afterwards:

$$cos\phi_{max} = \frac{k-1}{\sqrt{k^2.\frac{1}{\frac{k}{k+1}} + \frac{1}{1-\frac{k}{k+1}}}} = \frac{k-1}{k+1} \tag{2.34}$$

Chapter 3

CONTROL OF SYNCHRONOUS RELUCTANCE MOTOR

3.1 Introduction

In todays industrial world, electric machines are the most common power source for electricity. Therefore, saving energy from electric machines has been always a vital issue for the machine drive systems. Several numbers of problems about energy savings of electric machines have emerged. Therefore, plenty of studies are aiming to increase the efficiency of electric machines by minimizing the energy losses from every aspect in industrial applications [17]. Although there are some mechanical losses in electric machines due to rotational motion, most of the losses happens during the conversion from electrical to mechanical energy. Hence, the concept of efficiency can be expressed as;

$$Efficiency = \frac{OutputMechanicalEnergy}{InputElectricalEnergy}.100\% \tag{3.1}$$

Where;

$$OutputMechanicalEnergy = InputElectricalEnergy - MachineLosses \tag{3.2}$$

From the expression, it is possible to say that machine losses must be decreased in order to increase the output mechanical energy for a given input electrical energy. Consequently, the efficiency of the electric machine is improved [18].

There are different types of machine losses and the types of losses in an electrical machine are basically the same regardless of the type of machine such as copper losses, mechanical losses which include friction and windage losses, core and stray losses. In a three phase motor, the input power is the electrical power flow at the terminals. Power is then lost in the stator circuit, and the stator core. The remaining power is transferred to the rotor. Deducting the rotor losses, one obtains the power converted to the mechanical system. At this point stray losses and mechanical losses are deducted and the remaining power is the output power available to the mechanical load. In reality, core losses occur on both the rotor and stator and stray losses are usually electrical losses distributed throughout the motor. Core losses are allocated to the stator since this is where most of the core losses usually occur and stray losses must be taken off after the mechanical power is converted as it is not simple to include them in the electrical model.

Since the induction motor is the most popular machine in the industrial applications, decreasing the energy consumption of inductance machines has a considerable effect on the subject of energy sources savings. The efficiency of induction machines can be improved by using an adjustable or variable speed drive, so that induction motor losses can be reduced. Thanks to the fact that the voltage and frequency can be varied independently in adjustable speed drives, it provides a certain speed torque operating point which supplies maximum efficiency for different voltage frequency levels.

The concept of adjustable speed drives is also valid in permanent magnet synchronous motors (PMSM) and synchronous reluctance motors (SynRM). Since these motors have higher efficiency especially in fractional power rates, induction machines are gradually being phased out by these motors coupled with developing adjustable speed drives[19][20].

One of the reason of high efficiency in SynRM is that the origin of losses are reduced because there is no excitation winding on the rotor. However, the other losses that come from bearings, stator iron and stator conductor are substantially same with induction motor losses. Since the large scale of losses are caused by stator iron and conductor, optimizing the stator current has a great importance on increasing the efficiency of SynRM.

In the vector control of SynRM which is stated in first chapter, the field oriented control can manage the vector of stator currents, ids and iqs, independent from each other. That

enables the reluctance torque to vary with different levels of stator current vectors. For every given current vector pairs there is a particular motor torque characteristic, however, the efficiency of SynRM can change across a wide range. For instance, core losses are directly proportional to the d-axis current of the stator. That means in case of an increase in d-axis currents, the SynRM efficiency will decrease due to the increase of core losses at the stator. Although d-axis current can be minimized in order to satisfy the desired efficiency, the efficiency of the SynRM does not improve in a significant rate because q-axis currents increase the core losses in this case. However, there is an optimal operating point that the efficiency can be maximized by minimizing the core losses while the output torque of SynRM is still fulfilling the desired output torque. This optimal operating point refers to a pair (d-q currents) of current vector which is called maximum torque per ampere (MTPA) current. In addition, MTPA can also be identified as the current vector leads maximum torque with a constant magnitude. The MTPA point can be evaluated by using a model of a SynRM.

According to the researchers, using vector control methods such as field oriented control and direct torque control with embedded MTPA controller is the most appropriate option in order to operate with SynRM with higher efficiencies [21].

On the other hand, sensorless speed drives also produce an efficient control characteristic for SynRM. Sensorless speed drives are able to improve the reliability of the system while reducing the cost of the drive system [22].

Sensorless speed drives can be investigated in two categories. Initially, the voltage and the current are measured from the machine and speed can be estimated according to the measurements. Drives with this concept are named as speed sensorless control systems. Secondly, it is possible to derive reference current value by using two voltage sensors and one speed sensor and frequency of the motor can be varied according to it for maintaining the synchronism [23].

In this chapter, firstly, theory of a PI-based sensorless SynRM control system is investigated. Then, the tested drive system is explained with simulation block diagrams. Secondly, a field oriented control system which is combined with a MTPA algorithm is investigated after a short review of MTPA definition. Afterwards, a block diagram of the

simulation model is presented.

3.2 Sensorless SynRM Drive

This part illustrates a PI-based sensorless SynRM drive system. A short review of the concept is presented and the control system with a speed sensor is constructed to operate with SynRM.

3.2.1 Definition of Sensorless Theory

The theory of sensorless control is based on reducing the number of the sensors in the system in order to increase the reliability of the system. In this case, a speed sensor is employed and measured speed is compared with desired speed to estimate the input voltage for SynRM. Thus, current sensors and voltage sensors are dismounted from the system. The limitation of system is depend on the difference between measured speed and desired speed because voltage estimator has the input from that difference. If there will be a high difference between measured speed and desired speed, it will result with excessive amount of current at the stator. Therefore, the difference cannot be higher than equivalent maximum stator current.

Therefore, firstly, a d-q voltage estimator block has to be designed to supply an input to the SynRM. Since the drive system does not have a current sensor, voltage estimator should be able to create d-q voltages without using any current magnitude. Moreover, for the most efficient operation, the MTPA point has to be fulfilled with the reference voltage. When the MTPA point is reached, the current vectors, i_{ds} and i_{qs}, are equal to each other.

From the torque equation presented in equation 2-7, the current vectors can be derived as;

$$i_{ds} = \sqrt{\frac{T_e}{\frac{3}{2}.\frac{P}{2}.(L_{ds} - L_{qs}.)}} \tag{3.3}$$

$$i_{qs} = \sqrt{\frac{T_e}{\frac{3}{2}.\frac{P}{2}.(L_{ds} - L_{qs}.)}} \tag{3.4}$$

After that, when the equations 3-2 and 3-3 are substituted into d-q voltage equations, the voltage equations for the estimator can be obtained as shown below.

$$V_{ds} = (R_s + \frac{dL_{ds}}{dt} - \omega_r.L_{qs}).(\sqrt{\frac{T_e}{\frac{3}{2}.\frac{P}{2}.(L_{ds} - L_{qs}.)}}) \tag{3.5}$$

$$V_{qs} = (R_s + \frac{dL_{qs}}{dt} + \omega_r.L_{ds}).(\sqrt{\frac{T_e}{\frac{3}{2}.\frac{P}{2}.(L_{ds} - L_{qs}.)}}) \tag{3.6}$$

According to equations 3-5 and 3-6, it is possible to construct a d-q voltage estimator which is shown in figure 3.1.

3.2.2 Tested Sensorless Speed Controller Block Diagram

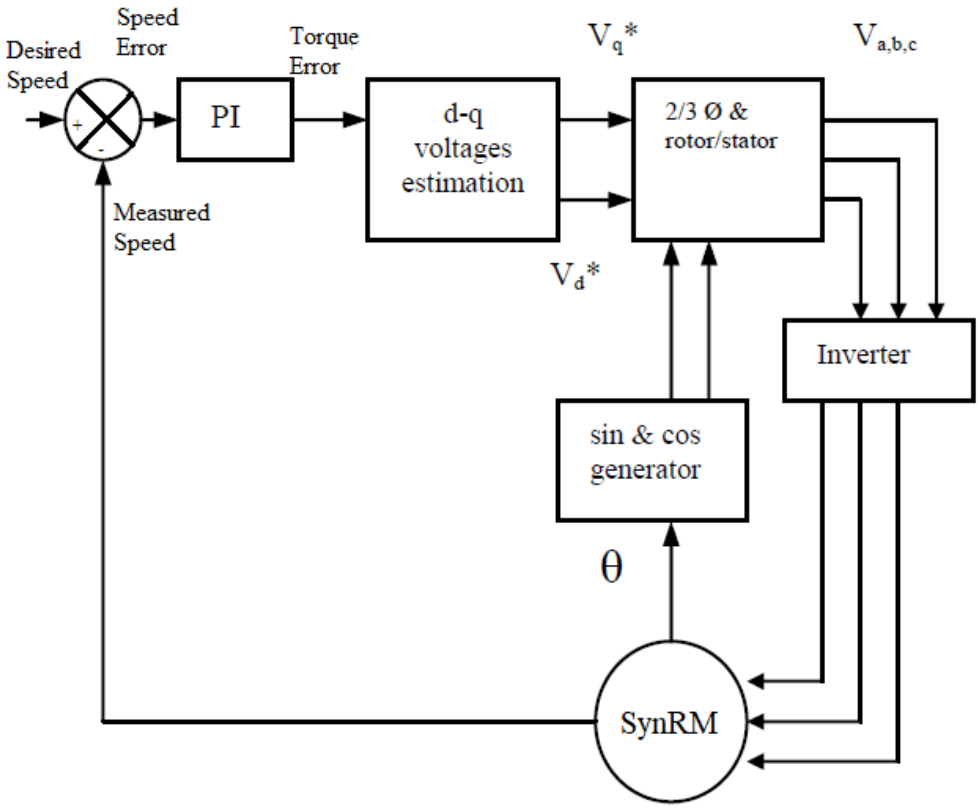

Figure 3.1: Sensorless SynRM Drive System Block Diagram

As it can be seen in figure 3.1, the d-q input voltages of the SynRM are derived by the difference of desired speed and measured speed from speed sensor which is also called speed error. After the speed error is determined, it is possible to convert it to torque error by integrating it. In this step of the system, the behavior of the motor can also be arranged by changing the integral coefficients of PI controller. The motor parameters ($L_d, L_q, R_s and P$) are constant and given in appendix and when torque error (T_e) is derived from PI controller, V_d and V_q voltages can be calculated from the estimator block which includes equations 3-5 and 3-6. Then, the 2 phase reference frame is transformed into 3 phase frame by using Park and Clarke Transformations in order to control the inverter. Closed-loop system is completed successfully when the inverter feeds the SynRM.

3.2.3 Simulink Model of Sensorless Speed Controller

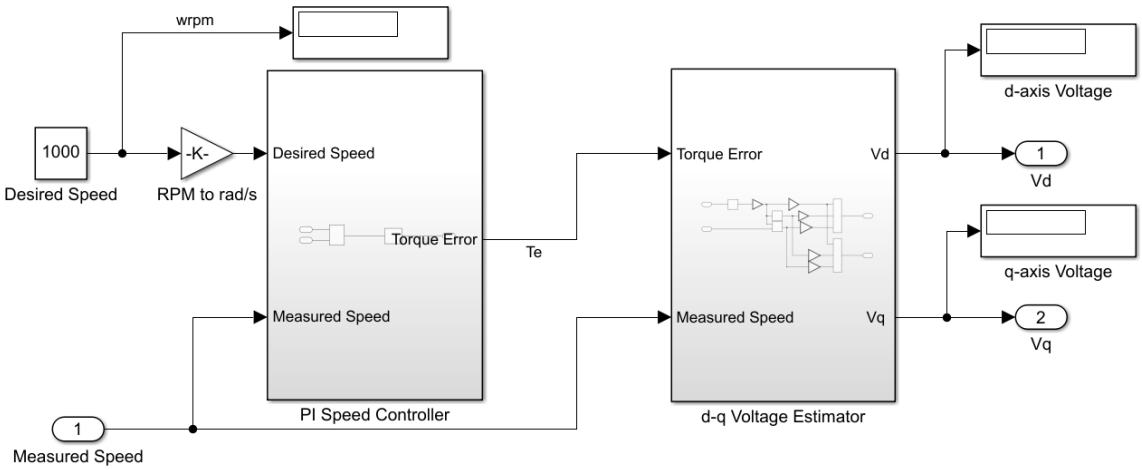

Figure 3.2: Sensorless Drive System Simulink Block Diagram

As the sensorless control theory which is explained in the previous section is constructed by using MATLAB/Simulink. The voltage equations showed in 3-5 and 3-6 are implemented as shown in figure 3.3.

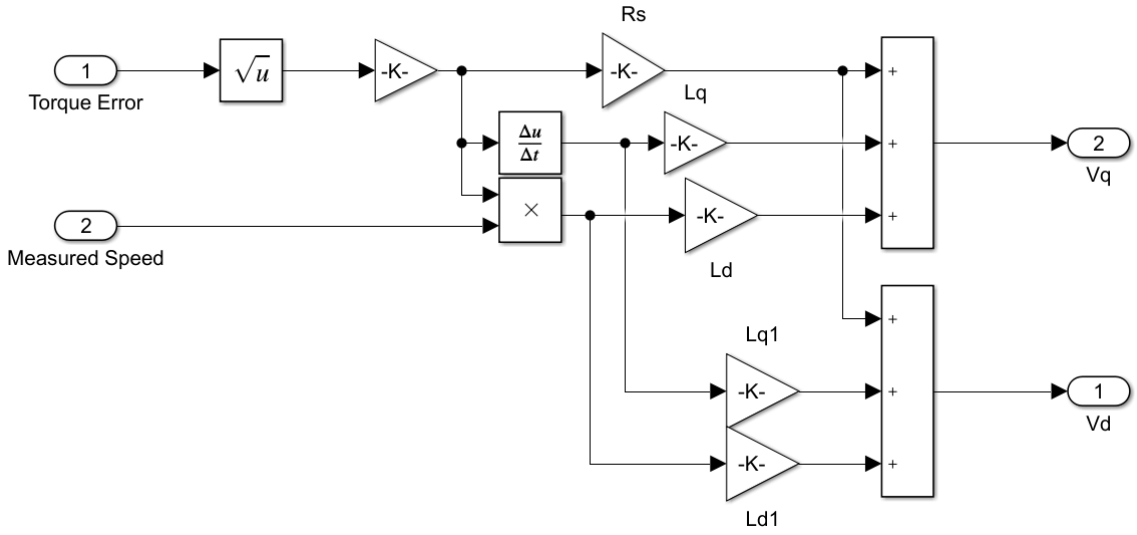

Figure 3.3: d-q Voltage Estimator Block

3.3 Maximum Torque per Ampere (MTPA) Control Theory

3.3.1 Definition of MTPA Theory

In the introduction part of the third chapter, it is stated that vector control models are able to control d-q axis stator currents independently and current vectors can be fixed at an operating point that gives the best efficiency rate. The name of this method, maximum torque per ampere, comes from its theory because this method tries to supply maximum torque for the given current vectors at the optimal operating point. The operating point can be determined from the operating characteristic graph of SynRM which illustrates the current and voltage limit equation together in the current plane ($i_d$vsi_q). Voltage and current limit equations which are shown in equation 3-7 and 3-8 are necessary to apply field oriented control and direct torque control methods.

$$I_{S,max}^2 = i_{ds}^2 + i_{qs}^2 \tag{3.7}$$

$$V_{S,max}^2 = V_{ds}^2 + V_{qs}^2 \tag{3.8}$$

Where;

$$V_{ds} = R_s.i_{ds} + L_{ds}.\frac{di_{ds}}{dt} - \omega_r.L_{qs}.i_{qs} \tag{3.9}$$

$$V_{qs} = R_s.i_{qs} + L_{qs}.\frac{di_{qs}}{dt} + \omega_r.L_{ds}.i_{ds} \tag{3.10}$$

The limit equation of current (3-7) represents a circle in the analytical plane with a radius of $I_{S,max}^2$ describes the maximum allowed current. Correlatively, voltage limit equation can be also plotted into operating characteristic graph by substituting d-q axis currents into equation 3-8 because the axes of graph are I_{ds} and I_{qs}.

Since, the derivative terms in the voltage equations 3-9 and 3-10 are zero at the steady state and resistive losses are negligible because the losses are too smaller than back electromotive force. Therefore, the voltage equation can be rewritten as [24]:

$$V_{S,max}^2 = (-\omega_r.L_{qs}.i_{qs})^2 + (\omega_r.L_{ds}.i_{ds})^2 \tag{3.11}$$

$$V_{S,max}^2 = \omega_r^2.L_{qs}^2.i_{qs}^2 + \omega_r^2.L_{ds}^2.i_{ds}^2 \tag{3.12}$$

$$1 = \frac{\omega_r^2.L_{qs}^2.i_{qs}^2}{V_{S,max}^2} + \frac{\omega_r^2.L_{ds}^2.i_{ds}^2}{V_{S,max}^2} \tag{3.13}$$

$$1 = \frac{i_{ds}^2}{\frac{V_{S,max}^2}{\omega_r^2.L_{ds}^2}} + \frac{i_{qs}^2}{\frac{V_{S,max}^2}{\omega_r^2.L_{qs}^2}} \tag{3.14}$$

$$1 = \frac{i_{ds}^2}{x} + \frac{i_{qs}^2}{y} \tag{3.15}$$

Where $x = \frac{V_{S,max}^2}{\omega_r^2.L_{ds}^2}$ and $y = \frac{V_{S,max}^2}{\omega_r^2.L_{qs}^2}$. The equation 3-15 is an eclipse equation with vertex y and co-vertex x where $y > x$. As a result, limitations for current and voltage can be

drawn on the same plot and their intersection point at the positive side plot demonstrate the MTPA point as shown in figure 3.4 [25].

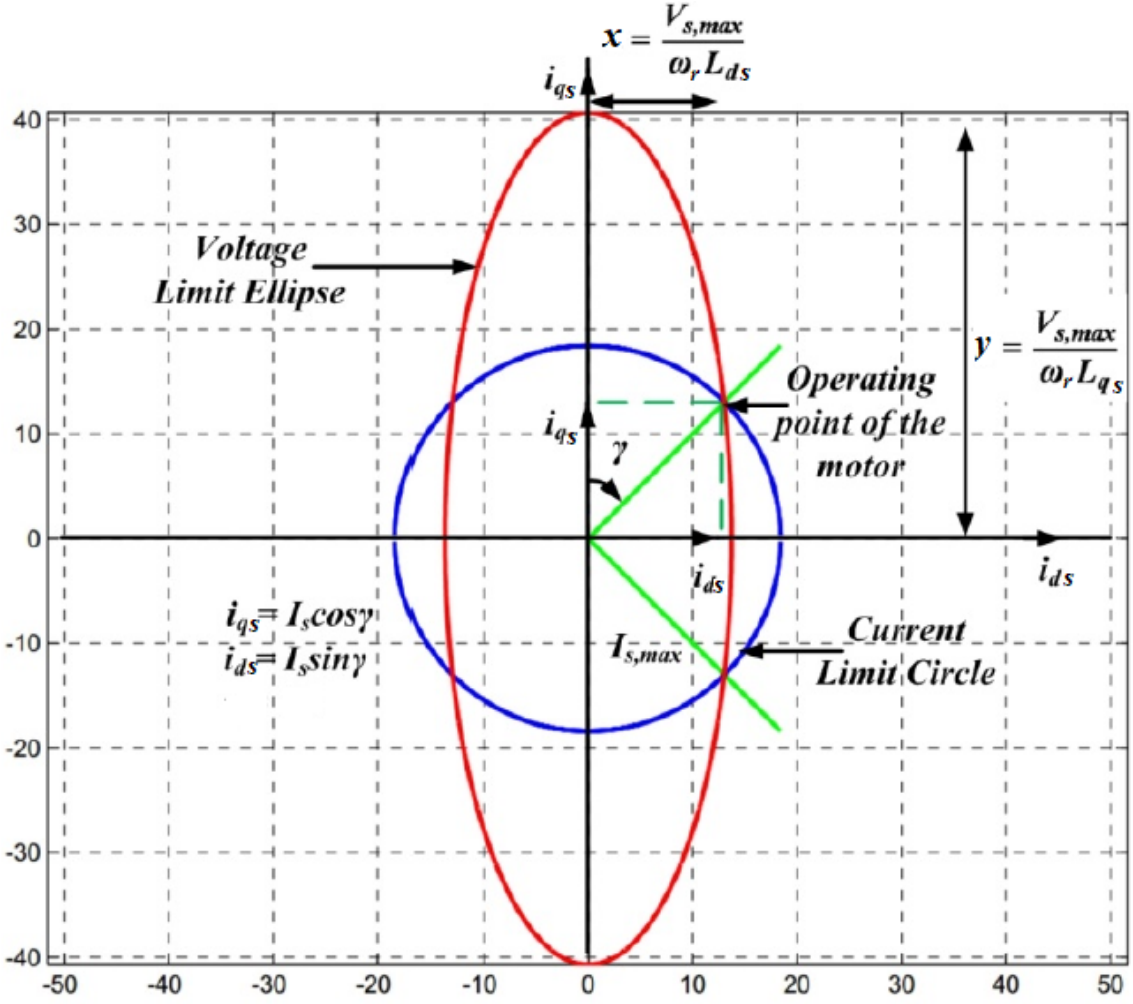

Figure 3.4: Operating Characteristics of SynRM [33]

As can be seen in the above operating characteristics graph, the intersection point of limitations is on the $I_{ds} = I_{qs}$ line. That explains why the MTPA point requires the condition of $I_{ds} = I_{qs}$. Mathematically, the MTPA point can be derived from the torque equation (3-16) of SynRM as shown below.

$$\tau_e = \frac{3}{2}.\frac{P}{2}.(L_{ds} - L_{qs}).i_{qs}.i_{ds} \tag{3.16}$$

Where

$$i_{ds} = I_S.sin\gamma \tag{3.17}$$

$$i_{qs} = I_S.cos\gamma \tag{3.18}$$

Since the motor parameters, P, L_{dq}, L_{qs} and R_s are unchangeable; a constant C can be assigned to simplify the calculation. When equations 3-17 and 3-18 are substituted into 3-16, the torque equation becomes;

$$\tau_e = C.I_S^2.sin\gamma.cos\gamma \tag{3.19}$$

$$\tau_e = C.I_S^2.\frac{sin2\gamma}{2} \tag{3.20}$$

Where $C = \frac{3}{2}.\frac{P}{2}.(L_{ds} - L_{qs})$.

Then, condition of MTPA can be applied as,

$$\frac{d\tau_e}{dt} = C.I_S^2.\frac{cos2\gamma}{2}.2 \tag{3.21}$$

$$cos2\gamma = 0 \tag{3.22}$$

$$\gamma_{MTPA} = 45^\circ \tag{3.23}$$

As a result, under MTPA condition the torque equation can be written as;

$$\tau_e = C.I_S^2.\frac{1}{2} \tag{3.24}$$

Then, d-q axis stator current equations become;

$$i_{ds} = I_S.sin45 = I_S.0,707 \tag{3.25}$$

$$i_{qs} = I_S.cos45 = I_S.0,707 \tag{3.26}$$

3.3.2 Tested MTPA Block Diagram

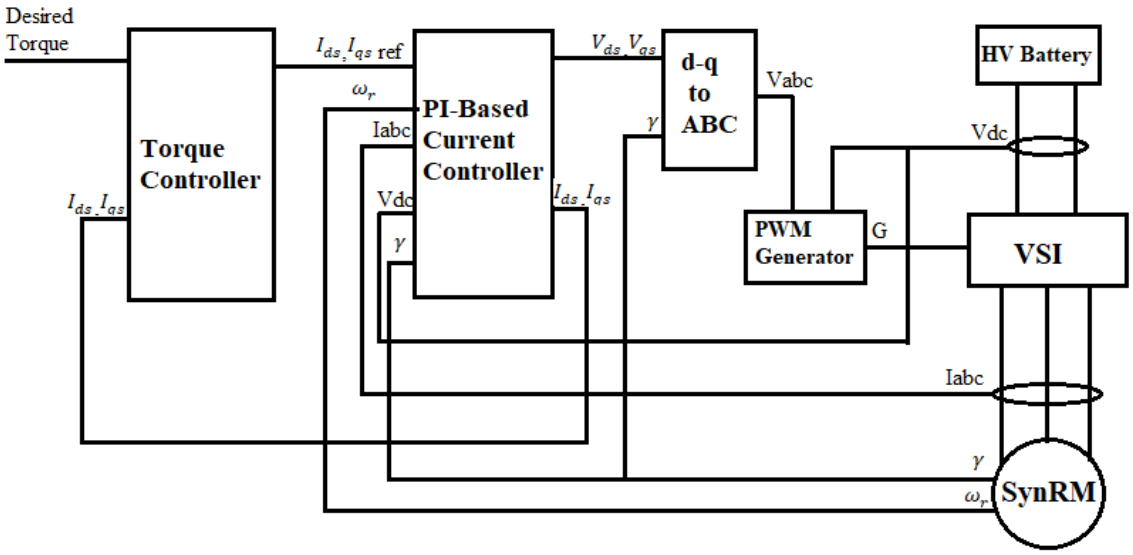

Figure 3.5: Field Oriented Control Based MTPA for SynRM

Figure 3.5 illustrates the block diagram of the tested MTPA scheme for SynRM. The control system uses an open-loop approach to control the torque and a closed-loop approach to control the current. The reference magnitude of the stator currents, i_{ds} and i_{qs} are decided through the torque controller from the desired torque. Then, stator reference currents are processed in the PI-based current controller which is MATLABs PMSM current controller. Current controller supplies the current and voltage vector magnitudes at their intersection point on the characteristics graph of SynRM as explained in the figure 3.4 and consequently MTPA operation is realized for desired torque.

At each sample instant, the desired torque is converted to relevant current references using the maximum torque per Ampere strategy. Stator current feeds back the torque controller in order to plot estimated torque graph. To validate the accuracy of the produced torque of SynRM, the estimated torque graph is necessary. The other output of the PI-based current controller is voltage vectors which are transformed into 3 phase frame by using Park and Clarke Transformation. PWM generator block is controlling the gate voltages of voltage source inverter by using these 3 phase voltages. The VSI is fed by an HV battery as an energy source for the SynRM. At the input of the SynRM, current sensors measure the 3 phase current and send it into the current controller where it is transformed to d-q frame by using inverse Park and Clarke Transformations in order to compare with reference stator current vectors. At the output of the SynRM, there are 2 sensors which measure current phase angle for Park and Clarke Transformations and speed in radians per second to be used as input of the current controller.

3.3.3 Simulink Model of MTPA Control

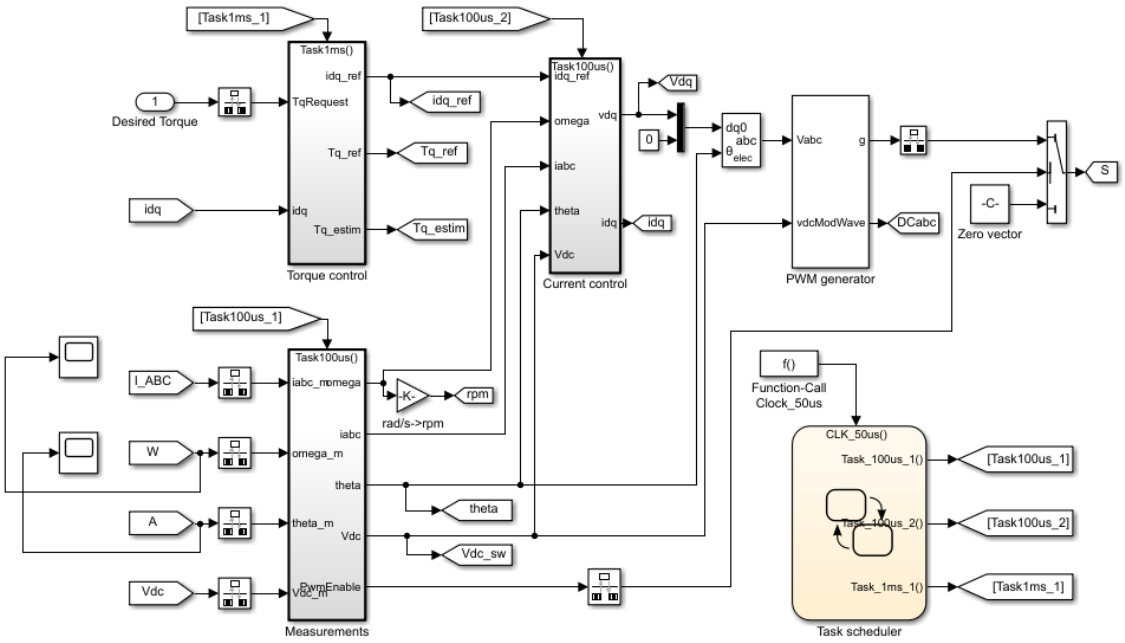

Figure 3.6: MTPA Control Block for SynRM in Simulink

The illustrated concept of theory is implemented in MATLAB/Simulink as shown in figure 3.6. Although the operation in principle is stated in the previous part, a clock block diagram is required as a task scheduler in order to simulate the model. The control block creates a simulation sample in every 50s. Current controller and torque controller operate in every 100s and 1ms, respectively. In other words, current controller sends 10 stator current vector samples for a single loop of torque controller to increase the accuracy of simulation. The rate transition blocks are used for every input to stabilize their sample time with the simulation time.

Chapter 4

SIMULATIONS AND RESULTS

4.1 Simulation Block Diagrams

4.1.1 Sensorless Speed Controlled SynRM

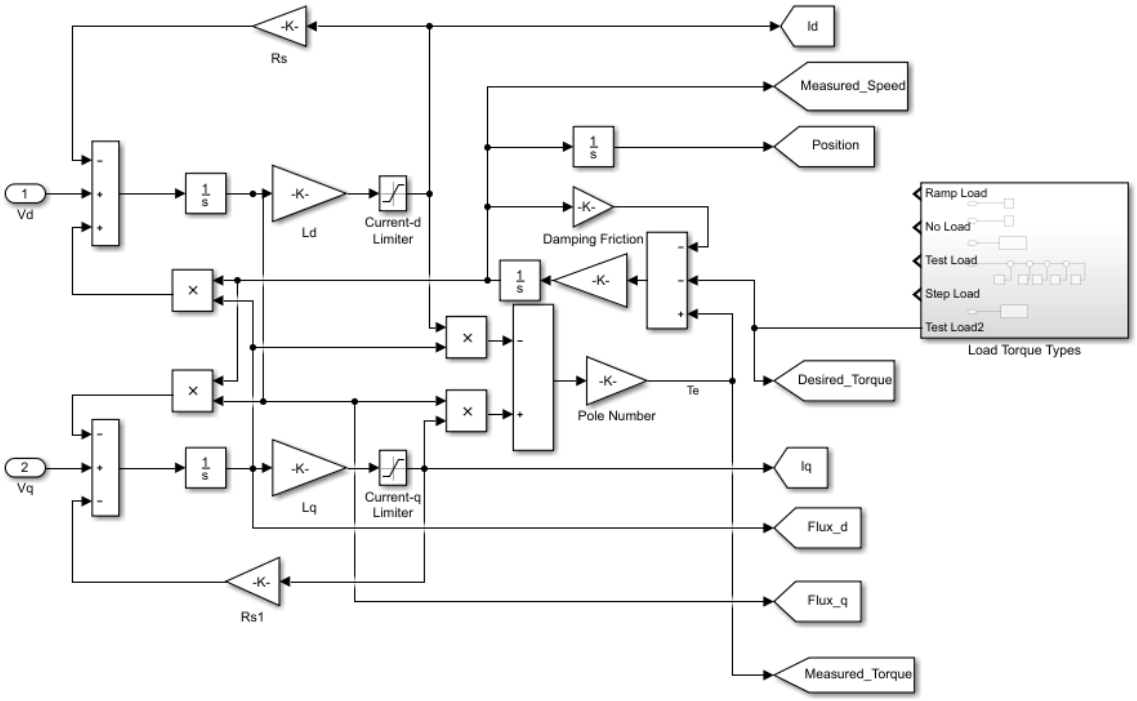

Figure 4.1: Simulink Block Diagram of SynRM in d-q Reference Frame

Due to its simpler structure, the SynRM is operated with sensorless speed control drive at first. There are several ways to design a SynRM in Simulink; however, the easiest and the most effective way is to design in the direct-quadrature-zero (dq0) reference frame which rotates with the rotor. According to the mathematical equations of SynRM, which are stated in chapter 2, the SynRM d-q frame model is constructed in Simulink as shown figure 4.1.

The d-q model of SynRM includes 4 different equations. These are: d and q voltage vector equations which are shown in 2-1 and 2-2, the torque equation stated in equation 2-7 and lastly the mechanical equation for the rotor which presents angular movement as shown in equation 4-1.

$$\tau_e - \tau_l = j.\frac{d\omega_e}{dt} + D_f.\omega_e \tag{4.1}$$

The outputs of voltage vector equations give the d-q axis current vectors and these current vector equations are placed into the electromagnetic torque equation to find the reluctance torque of rotor (T_e) Afterwards, when the electromagnetic torque is subtracted from load torque, the condition to find angular speed in radians per second is satisfied mathematically.

In addition, the magnitudes of current vectors are limited by the saturation block in Simulink in case of higher current production than the motor can drive, so that the motor will be protected from possible damages caused by excessive amounts of current. Moreover, few load torque types are defined such as no load, ramp load, step load and mixed in order to test the behavior of the motor in different circumstances.

At the output of the SynRM: d-q stator current and voltage vectors, d-q rotor fluxes, position of rotor, measured-desired speed, and lastly measured-desired torque graphs are observed. In order to simplify the block diagram a measurement block diagram is constructed which is shown in figure 4.2 and all the scopes for the outputs of the motor are placed inside of it.

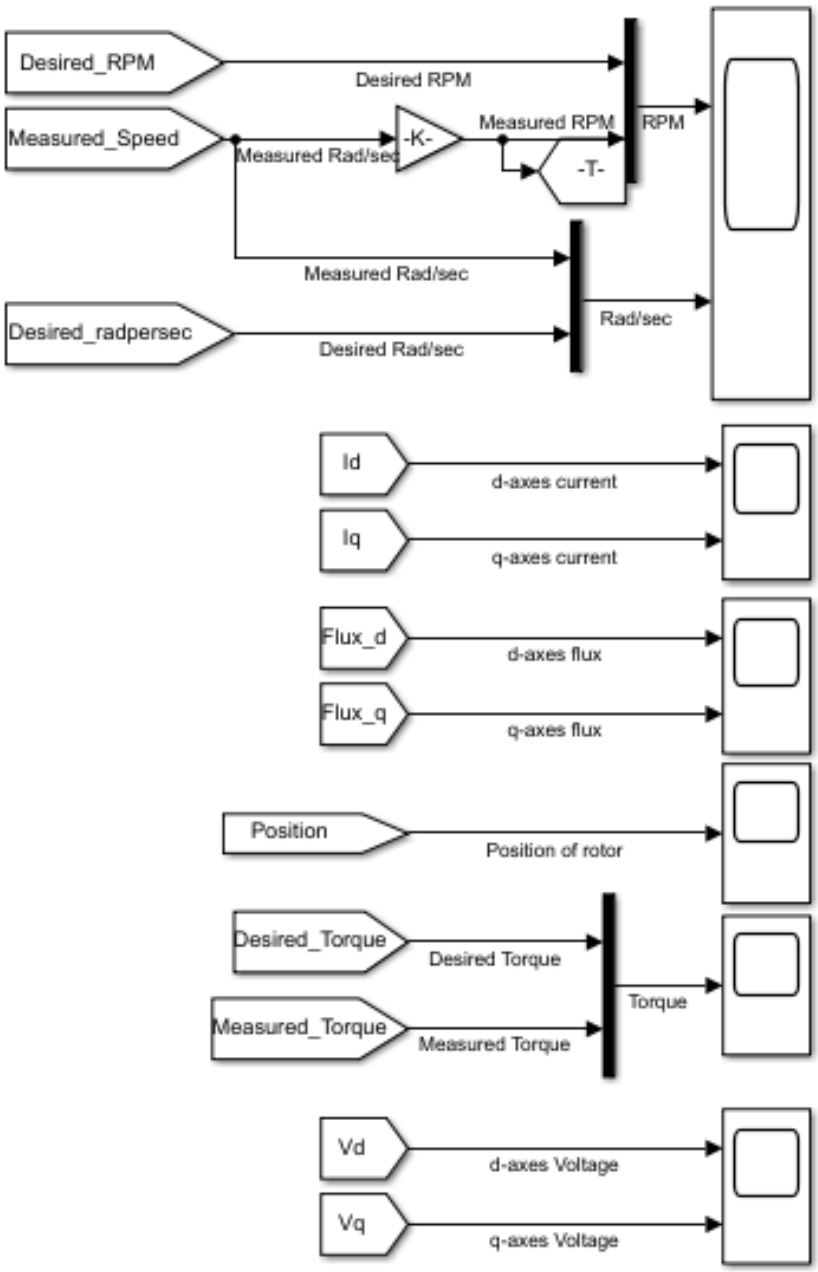

Figure 4.2: Measurement Block for the Outputs of SynRM

The voltage input for the motor block is supplied from estimator and sensorless speed controller. Speed controller and estimator arrange the input voltage of stator according to the feedback of the motor which shows the measured speed of the motor. For a better understanding of the whole simulation, a block diagram is presented in figure 4.3.

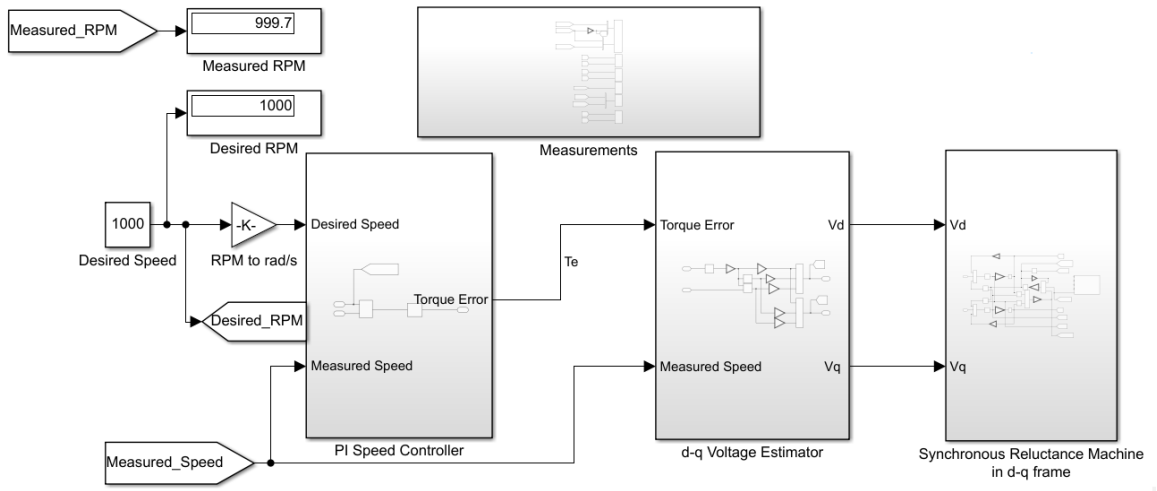

Figure 4.3: Synchronous Reluctance Motor with Sensorless Speed Controller

4.1.2 MTPA Controlled SynRM

In this part, one of the most widely preferred control methods for SynRM, which is called MPTA, is simulated by making use of MATLABs library. The main scheme of the system, SynRM inverter and source, is constructed by using Simscape library, but the control scheme is designed with the Simulink library. The control system is presented in chapter 3 and the complete block diagram is given below in figure 4.4.

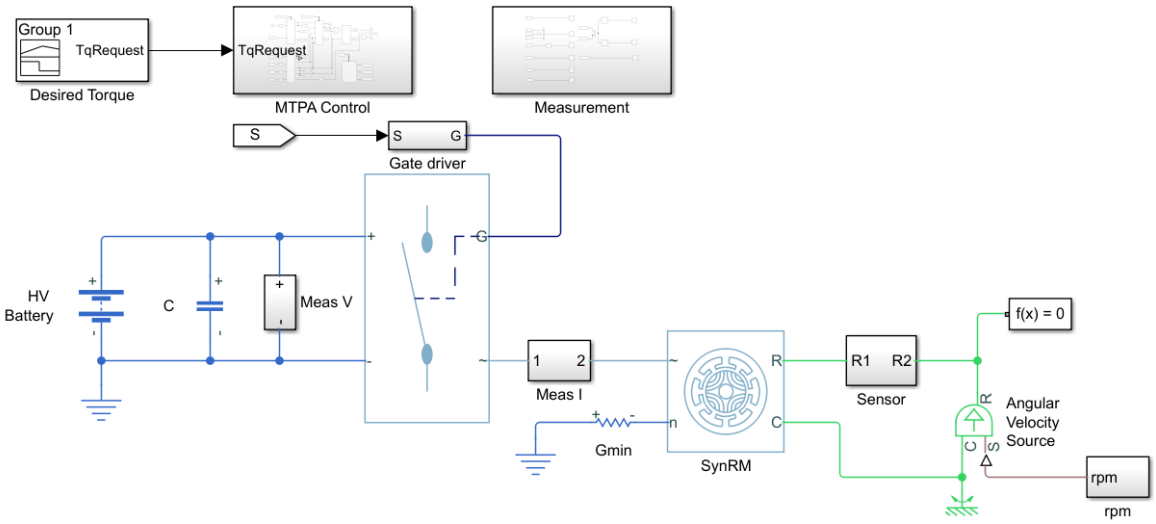

Figure 4.4: Simulation Block Diagrams for MTPA Controlled SynRM

From the motor, the current values are obtained by sensors and fed back to the MTPA controller. In the controller, the current value is varied to satisfy the desired torque by PI-based current controller. Then, the current controller supplies voltage to the inverter gates and controls the SynRM. The inverter is energized by a HV battery that is supplying 600 Volts. At the output of the motor, there is a sensor that measures torque, angular speed and current vector angle (ϕ)

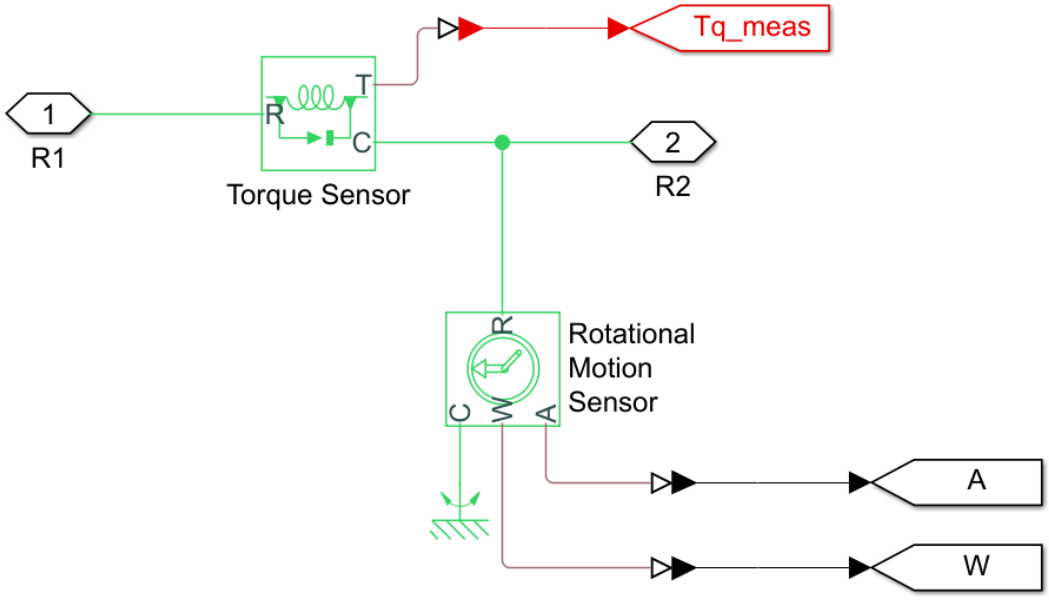

Figure 4.5: Sensor That Measures Torque, Angular Velocity and Current Vector Angle

In this simulation, the current vector angle is of great importance because the main circuit of the motor is in 3 phase reference frame; however, the control scheme is in d-q reference frame. This difference between systems requires Clarke and Park Transformations which cannot be done without current reference angle. For the outputs of the system, a measurement block is constructed similar to the previously explained sensorless speed drive simulation.

4.2 Results of Simulations

In this part, operating characteristics of the SynRM is investigated and all the results obtained from the SynRM are presented for both control cases with different load types. Afterwards, traction effort curve is explained and plotted for the simulated SynRM.

4.2.1 Results of Sensorless Speed Controlled SynRM

In this case two types of load, no load and mixed load types are used to examine the motor behaviors. Initially, no load case is set up and observed. In figure 4.6 and 4.7, the d-q voltages that feed the motor are presented.

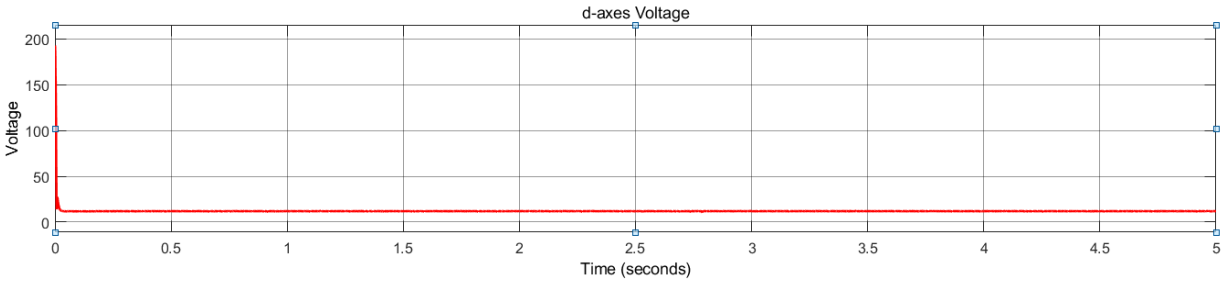

Figure 4.6: Input d Axis Voltage for SynRM in No Load Case

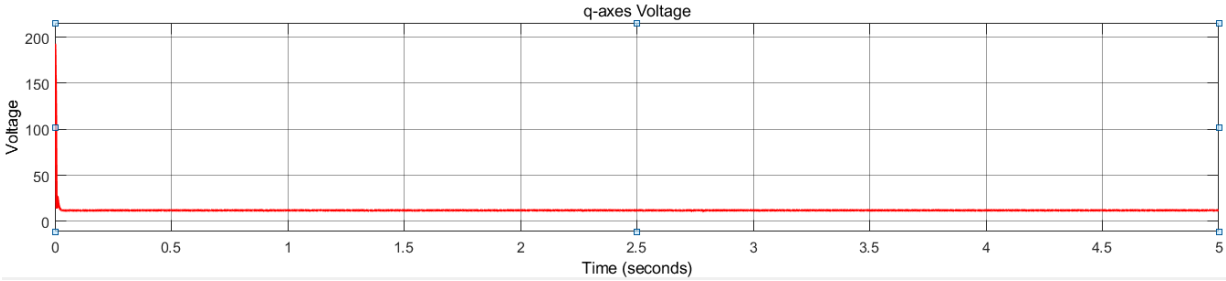

Figure 4.7: Input q Axis Voltage for SynRM in No Load Case

Input voltage energizes the motor by using 190 Volts and reduces to its minimum value which is 11Volts to keep motor running. Since there is no load torque that affects the motor, there is no need to increase the input voltage.Figure 4.8 and 4.9 show the d-q current magnitudes at the stator of the SynRM.

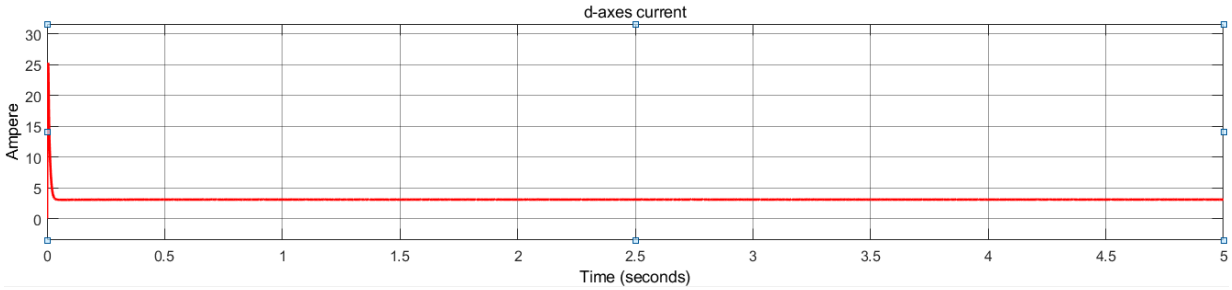

Figure 4.8: Stator d Axis Currents for SynRM

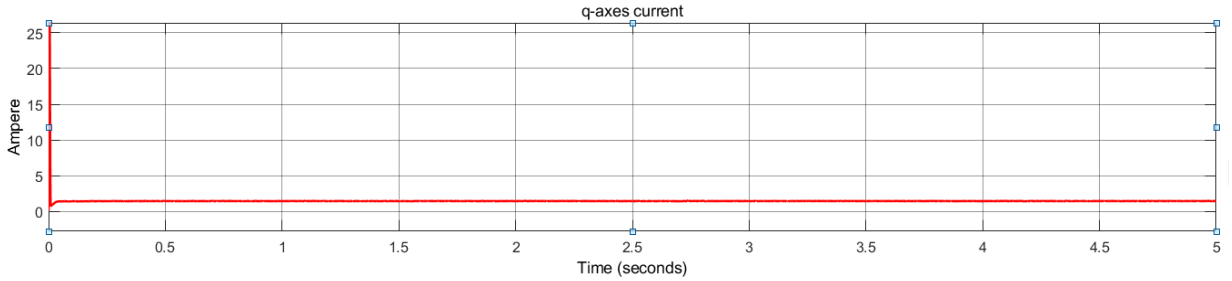

Figure 4.9: Stator q Axis Currents for SynRM

At the transient state, d axis current reaches 25A and q axis current is limited at 30A by saturation block to initialize the motor. Then, d and q axis currents stabilize at 3A and 1.1A respectively. Since the rotor fluxes are directly proportional to stator currents, the behavior of fluxes are similar with the stator currents as shown in figure 4.10 and 4.11.

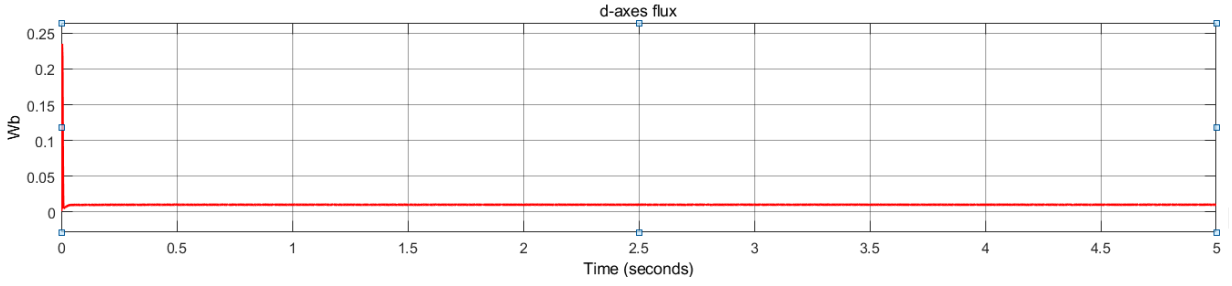

Figure 4.10: Rotor Fluxes in d Axis Reference Frame

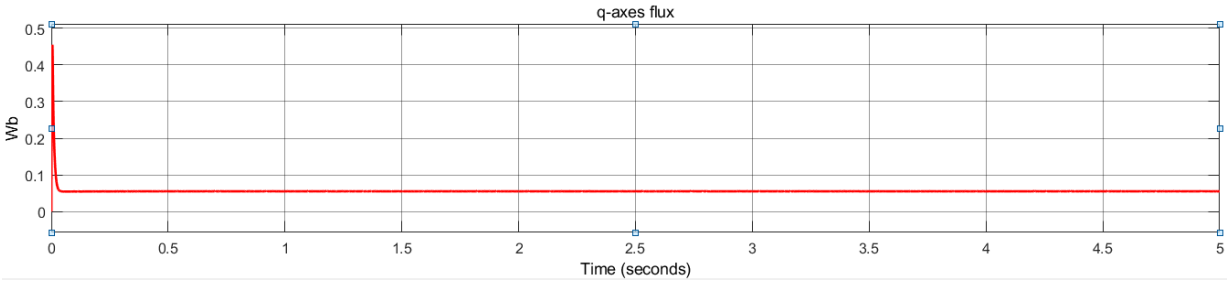

Figure 4.11: Rotor Fluxes in q Axis Reference Frame

The q-axis flux magnitude is almost half of d-axis flux magnitude in both steady state and transient state. With the measured current magnitudes, pole number and inductance values of the motor, the measured torque graph can be determined as follows;

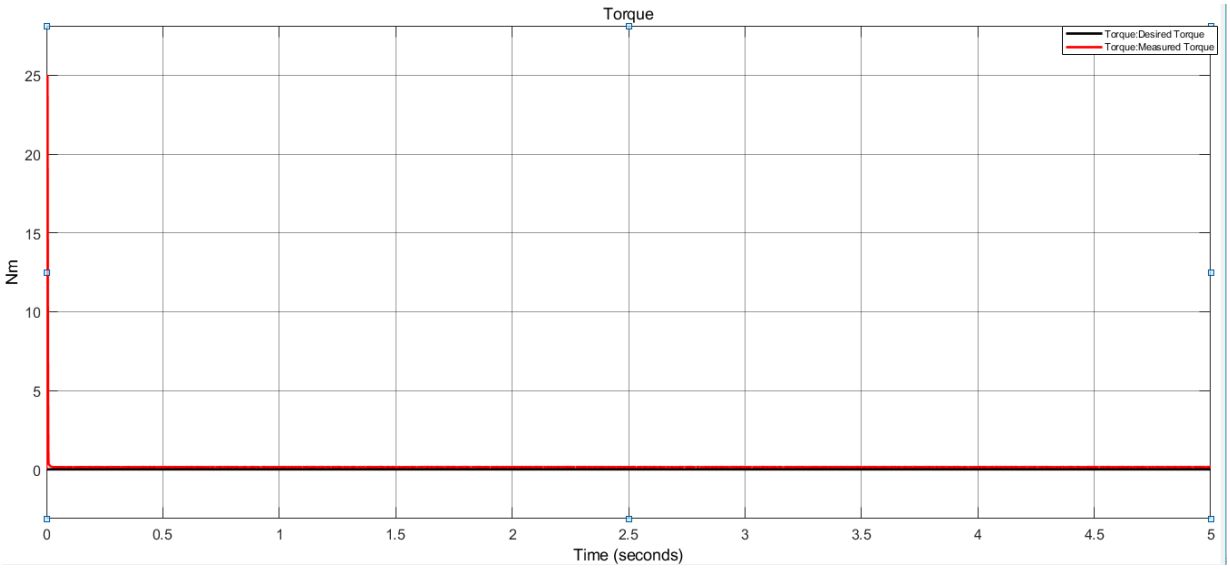

Figure 4.12: Measured Torque and Desired Torque Plot in No Load Condition

The red line shows the measured torque and it validates that the motor has no load torque. Measured torque is reaching 25 Nm to initialize the spinning of the motor and then satisfies the no load condition. When the torque output of the motor placed into the mechanical dynamic equation with moment of inertia and damping friction constant, the speed can be observed in radians per second as shown in figure 4.14. After that, speed is

multiplied by 60Hz/2pi to observe in revolution per minute as shown in figure 4.13. Since the desired speed is 1000rpm, measured speed is stabilized at 1000rpm in steady state.

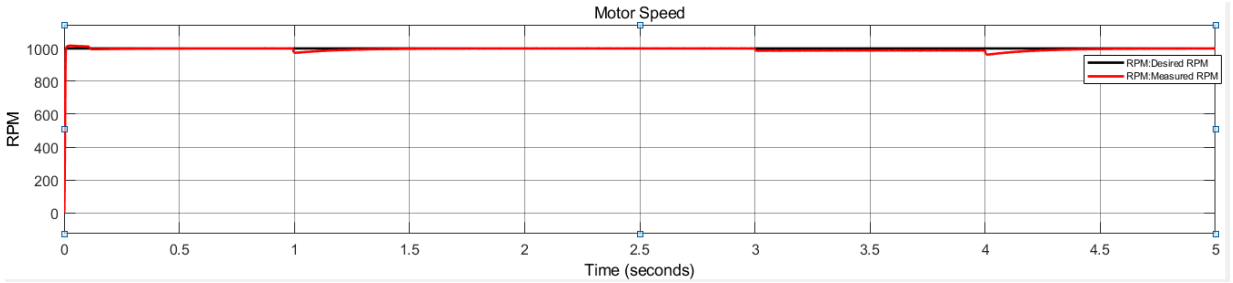

Figure 4.13: Motor Speed in RPM in No Load Condition

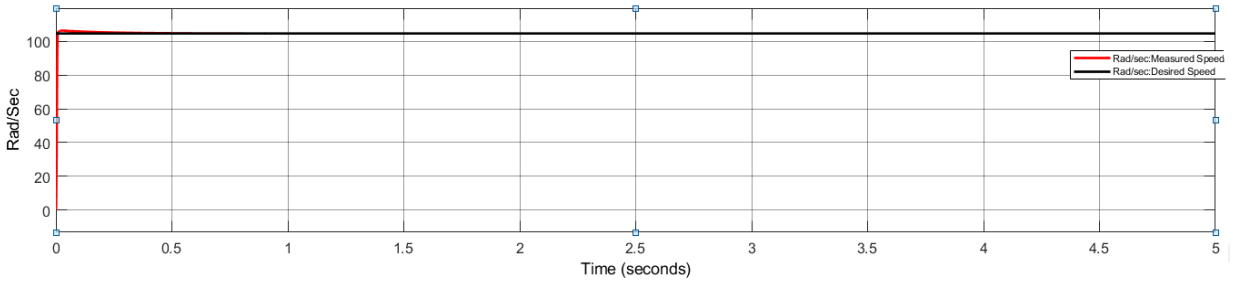

Figure 4.14: Motor Speed in radians per second in No Load Condition

In the second case, different load types are applied to the motor and same output measurements as the previous case are investigated. The desired torque which contains ramp load, step load and constant torque and the measured torque are shown in figure 4.15.

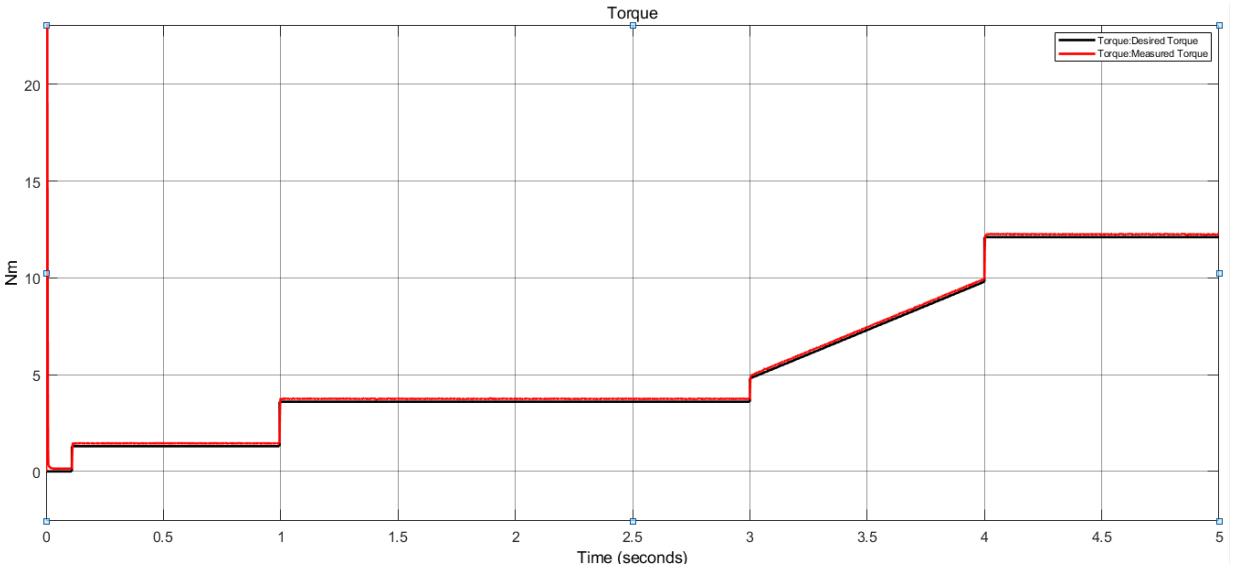

Figure 4.15: Measured and Desired Torque with Load Torque

The desired load torque is shown with the black line and the red line represents the measured torque. It is seen that the desired torque is perfectly satisfied by the measured torque.Moreover, the input voltage in d-q axis is also changed with the changing torque direct proportionally as shown in figure 4.16 and 4.17.

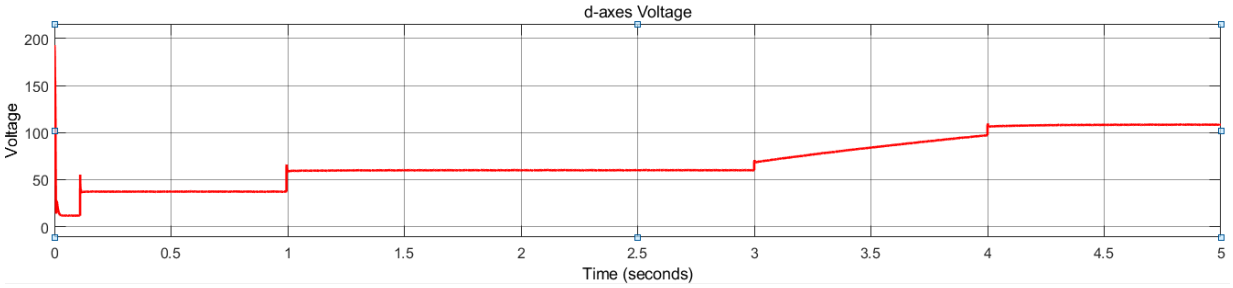

Figure 4.16: Input Voltages d Axis for SynRM with Load Torque

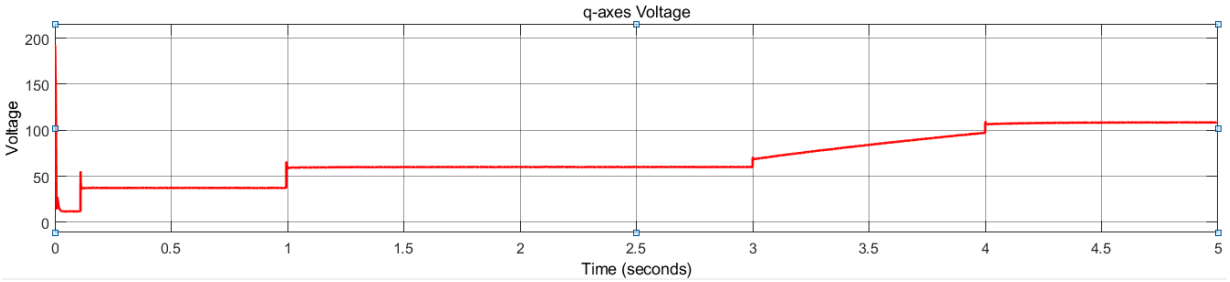

Figure 4.17: Input Voltages q Axis for SynRM with Load Torque

Similarly, stator current and rotor flux is affected by the change at the torque, as illustrated in figure 4.18,19 and figure 4.20,21 respectively.

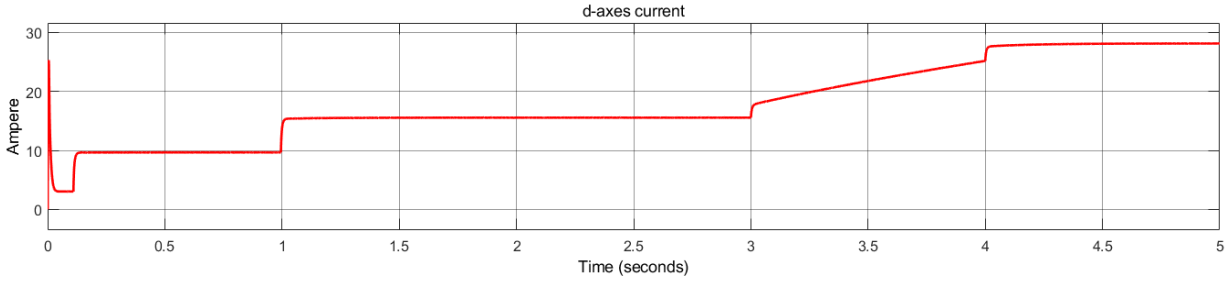

Figure 4.18: Stator Currents in d Axis Frame with Load Torque

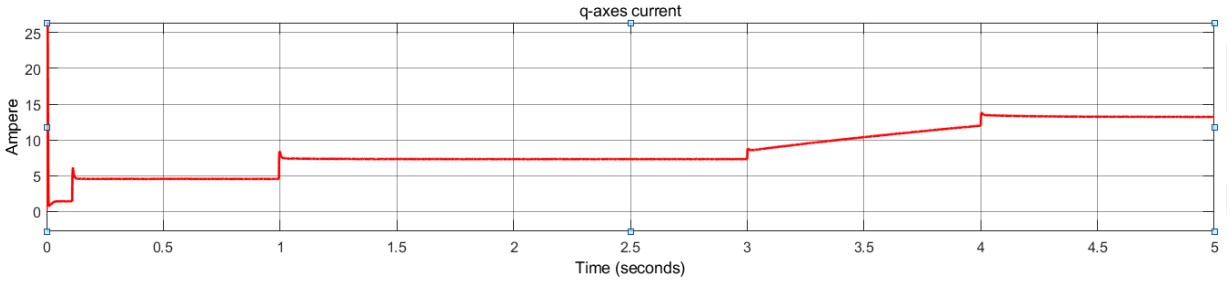

Figure 4.19: Stator Currents in q Axis Frame with Load Torque

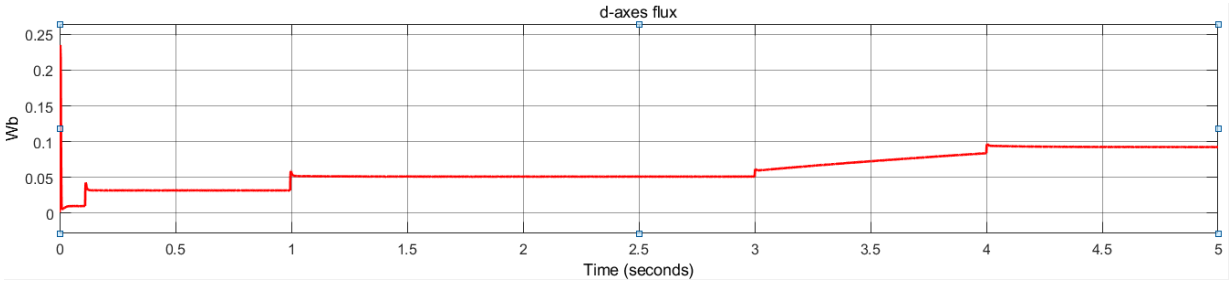

Figure 4.20: Rotor Fluxes in d Axis Frame with Load Torque

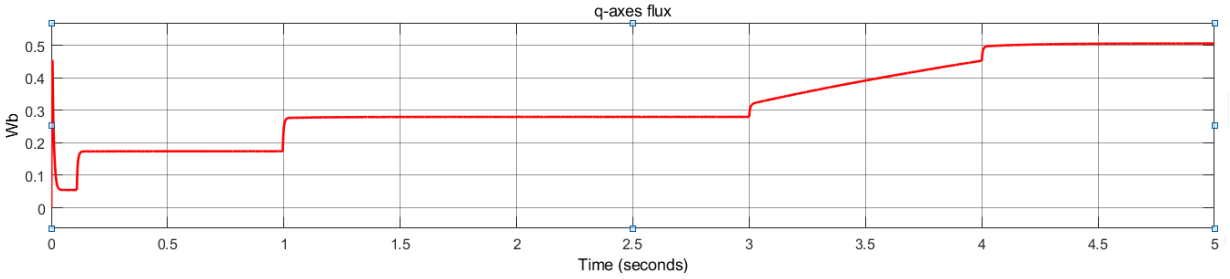

Figure 4.21: Rotor Fluxes in q Axis Frame with Load Torque

In accordance with the previous case, the d axis current is relatively higher than q axis currents. Also, the behavior of fluxes are similar with the no load torque case which means the q-axis fluxes magnitudes are double of the d-axis fluxes magnitudes.

In the synchronous motors, independent from the load torque, the synchronous motors speed does not change and this can be observed in the figure 4.22.

Figure 4.22: Desired and Measured Speed with Load Torque

However, at the moment the load torque is varied, there exists a ripple in the magnitude of the motor speed. Then, the motor speeds stabilize back to the desired rpm value as shown in figure 4.23.

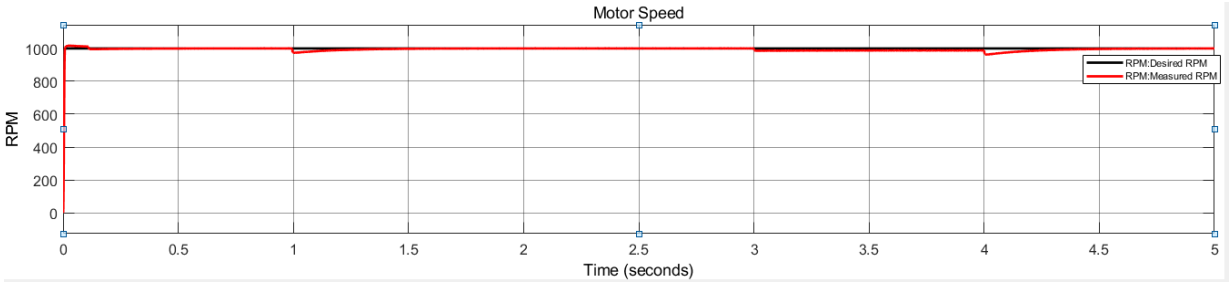

Figure 4.23: Measured Speed and Desired Speed in RPM of the SynRM under Load Torque Effect

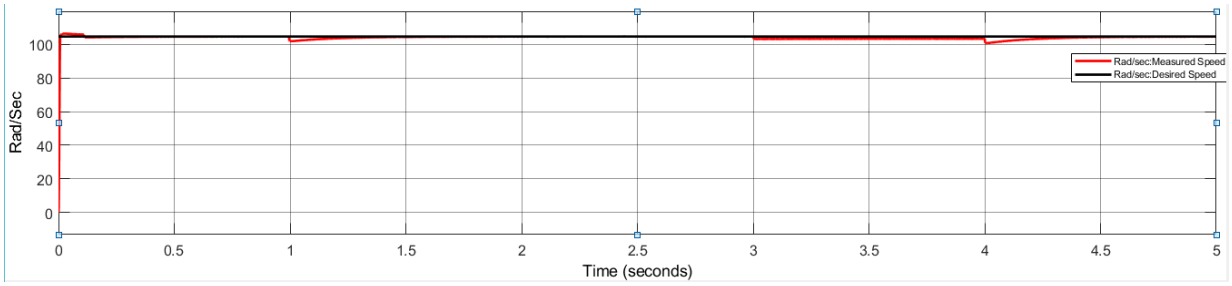

Figure 4.24: Measured Speed and Desired Speed in Radians per second of the SynRM under Load Torque Effect

In figure 4.24, the graph illustrates the speed in radians per second and above it is the same graph in revolutions per minute. Moreover, the position of rotor can be found by integrating the measured speed and it is demonstrated in figure 4.25.

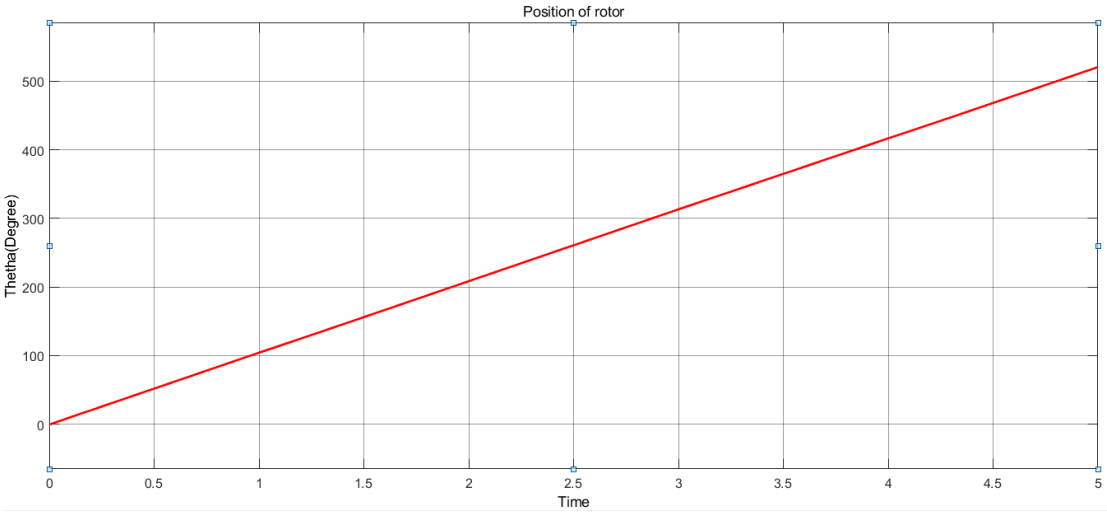

Figure 4.25: Position of the Rotor with a Load Torque

4.2.2 Results of MTPA Controlled SynRM

In this section, the results obtained with the MTPA controlled SynRM are given. A specific desired torque which includes ramp loads and step loads is defined like in previous simulation and requested from the motor with a signal builder block which is shown in the figure 4.26.

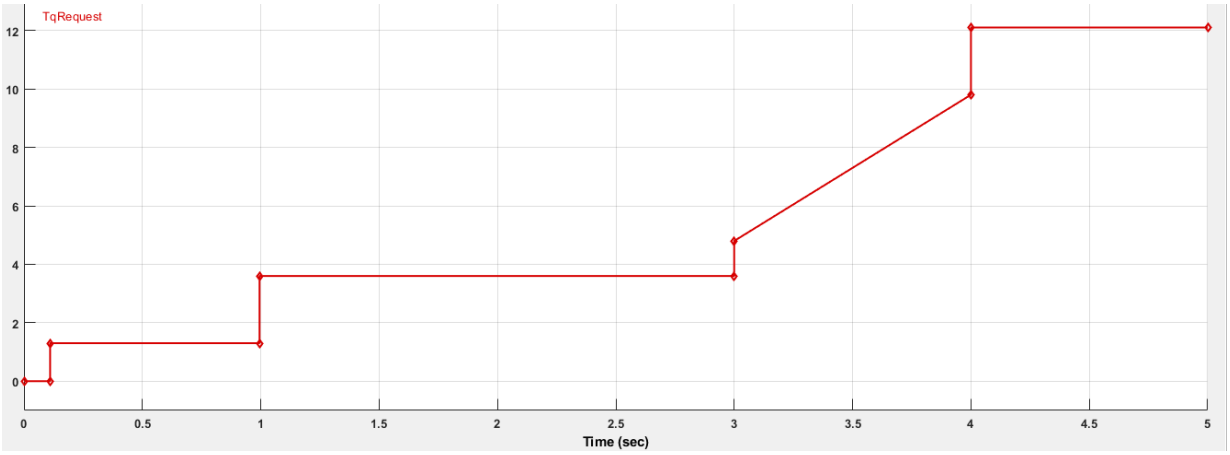

Figure 4.26: Desired Torque from the SynRM

Since the SynRM is fed by 3 phase current in this simulation, it is possible to observe

these 3 phase current's behavior against the demanded torque load as shown in figure 4.27.

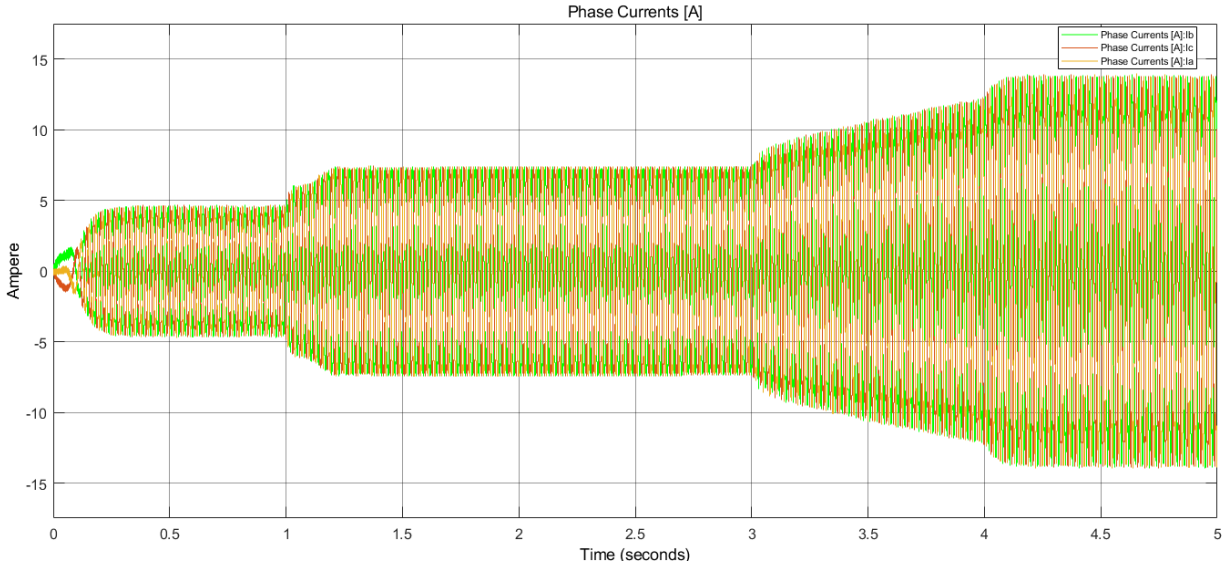

Figure 4.27: 3 Phase Currents feeding the SynRM

According to the 3 phase current graph, all phases of the current increase with the rise in the demanded torque. Moreover, highest current which changes between 14A and -14A is observed at the biggest demanded torque that is 13Nm. The d-q components of the current can be plotted by applying Park and Clarke Transformations. Moreover, the desired current value can be derived from the desired torque signal. Figure 4.28 and 4.29 show the measured and desired d-q current vectors.

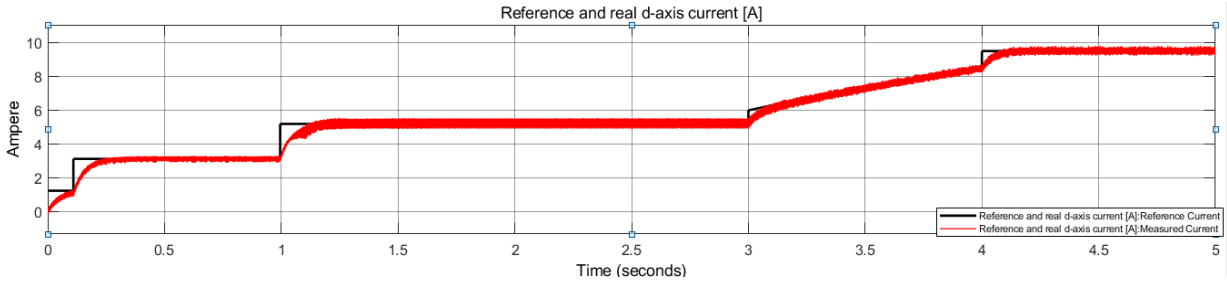

Figure 4.28: Stator Current Vectors in d Axis Reference Frame

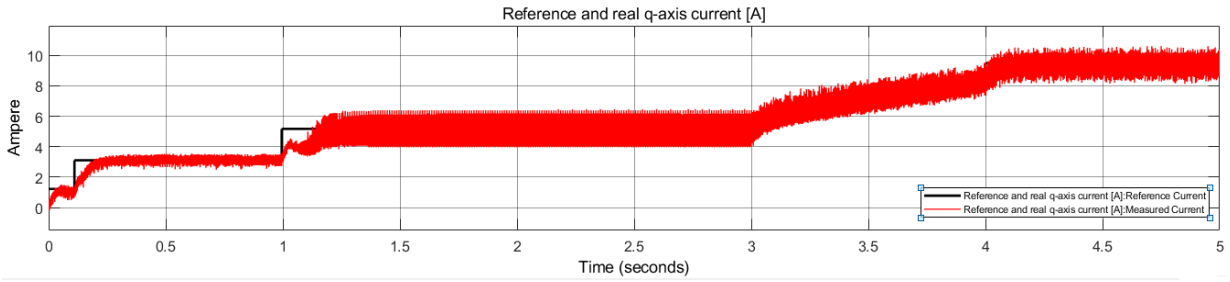

Figure 4.29: Stator Current Vectors in q Axis Reference Frame

In figure 4.29 and 4.28, the graphs show the measured and desired axis currents and it can be observed that the measured stator current values satisfy the desired current values. Both d-q axis stator currents increase with torque, but q axis currents have more oscillations than d axis currents when the torque is increased. MTPA method creates more oscillations on stator current and voltage plots than sensorless speed control because the MTPA point is checked in every 100ms as stated in previous chapter.

On the other hand, d-axis stator voltage has similar behavior with d-axis stator, but q-axis stator voltage does not increase as much as d-axis voltage. The axis voltage increases up to 80V with the applied torque on the SynRM, but q-axis voltage can rise up to 40V at the highest desired torque. The d-q voltage graph is given in figure 4.30.

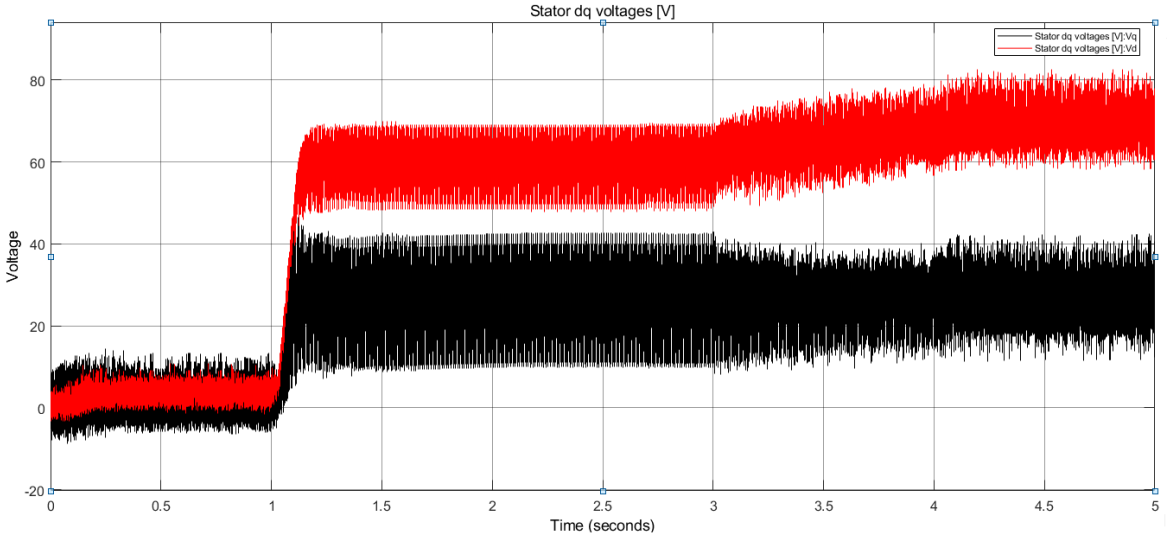

Figure 4.30: Stator Voltages in d-q Frame

Since this simulation contains a couple of Parks Transformations, the electrical rotor angle has vital importance for running the simulation accurately. It is measured with rotational motion sensor as shown in figure 4.31.

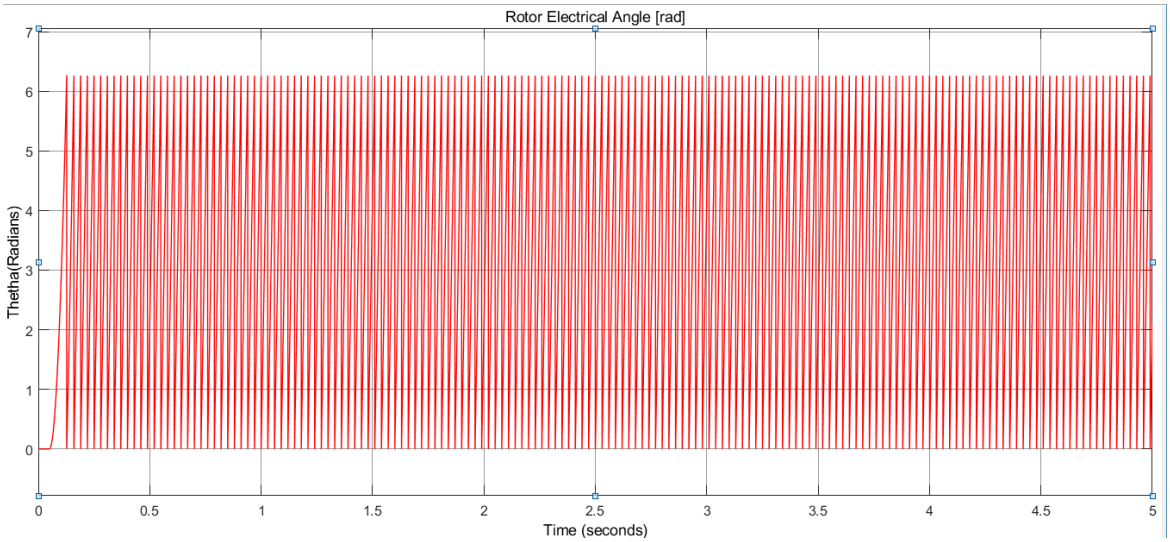

Figure 4.31: Rotor Electrical Angle in radians

As seen in the graph, the rotor electrical angle is not affected by the load torque and it changes between 0 and 2π. The rotor angle also gives information about its position since the rise 0 to 2π is equal to one revolution. From the graph, it can be commented that rotor is continuously spinning without any loss of moment even though there is a changing load torque affected on it.

In the simulation speed is arranged by an rpm load and for this simulation the given speed is 1000 rpm. Speed versus time graph is shown in figure 4.32.

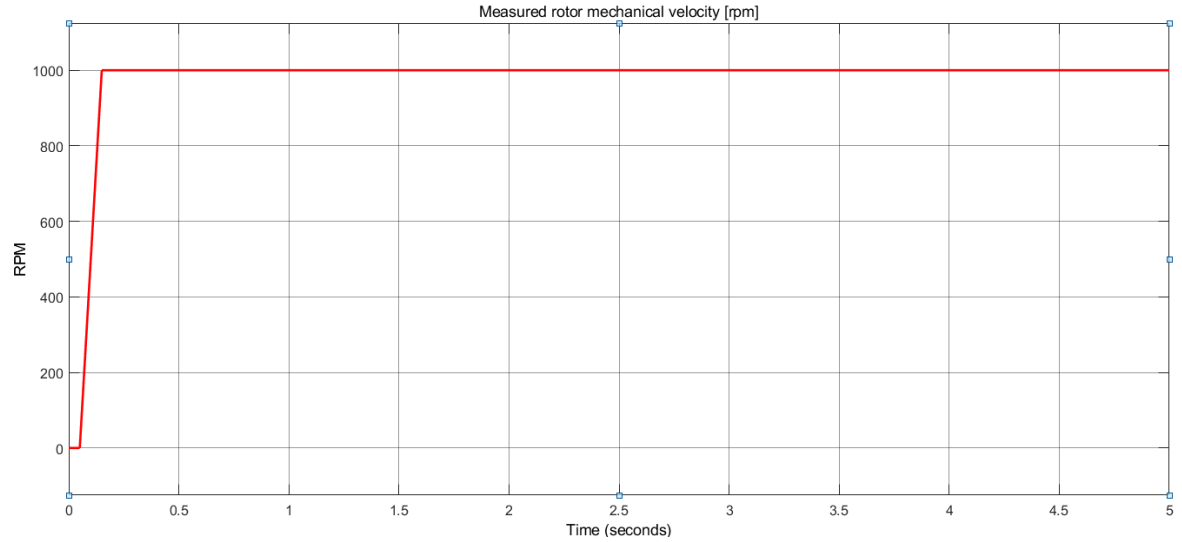

Figure 4.32: SynRM Speed in RPM With MTPA Control

MTPA control serves better speed quality than sensorless speed control which is illustrated in figure 4.33 because there is no ripple in the speed curve when the desired torque increases. On the other hand, if the desired torque is increased, there will be ripples on speed curve in sensorless speed control.

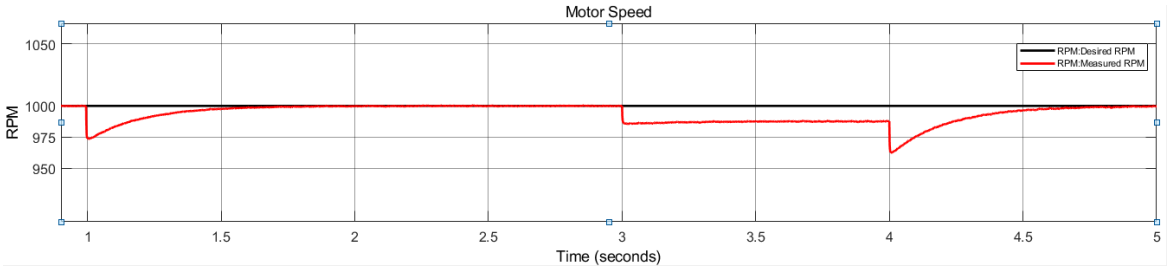

Figure 4.33: SynRM Speed in RPM With Sensorless Speed Control

PI-based current controller makes the estimated torque possible to calculate; therefore it can also be compared to the desired torque as shown in figure 4.34.

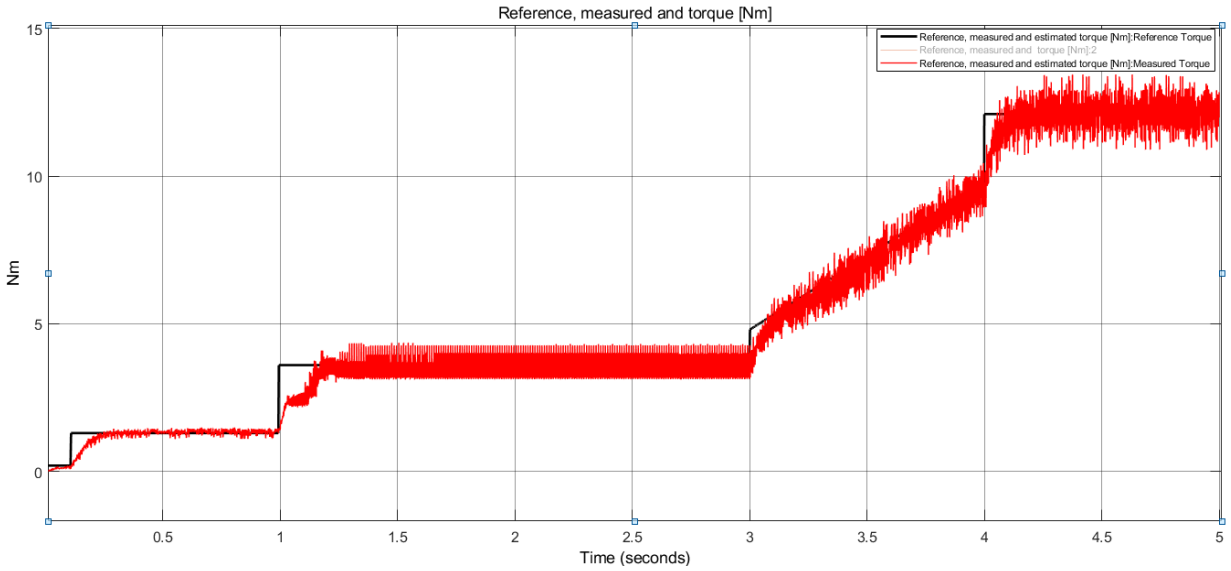

Figure 4.34: Measured and Desired Torque Graph

As it is seen in figure 4.34 the measured torque, which is shown by red color, satisfies the desired torque which is shown in black. Measured torque follows the desired torque lines with an exponential curve at the changes of load torque because of the motor's mechanical limits. When figure 4.33 and 4.15 are compared, it can be seen that sensorless speed control fulfills the desired torque better than MTPA control thanks to its fixed MTPA point.

4.3 Traction Effort Curve

Traction force identifies the total traction a vehicle exerts on a surface or the amount of the total traction which is parallel to the direct motion. Tractive effort describes the tractive force for fulling or pushing capability of a motor under a load torque. Generally, tractive force is defined as;

$$F_t = \frac{P}{\nu} \tag{4.2}$$

Where P is power, v is velocity and F is traction force. Tractive effort is inversely correlated with speed at any given level of available power. The tractive effort is shown with a graph which has the speed on x-axis and tractive force on y-axis and this graph is named as traction effort curve. An example of traction effort curve is shown in figure 4.35 to define the concept of the graph.

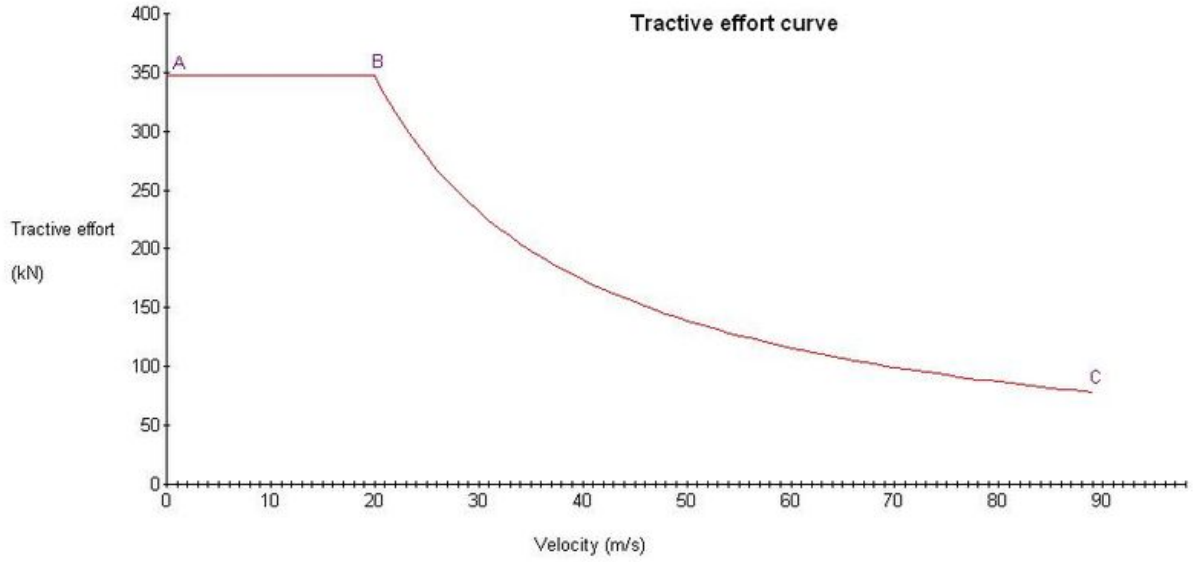

Figure 4.35: An Example of Traction Effort Curve

The example curve shows that the maximum torque of the motor is 350 kN and the maximum velocity is 90 m/s. The AB line at the top of the graph shows the operation at

the maximum tractive effort and the BC line shows the continuous tractive effort which is inversely correlated with speed. At point B the motor is at its nominal speed and at point C the motor is at its maximum speed. Since every motor has limitations on input current, the produced torque is limited. Hence, there exists linearity at the maximum tractive effort period. Consequently, the traction effort curve has a significant importance in railway and automotive industries because motors maximum loadability can be observed from the graph.

4.3.1 Traction Effort Curve of SynRM with Sensorless Speed Controller

For the different speed values maximum loadability is observed by applying a ramp torque. While the machine is rotating with constant speed, the load torque increased linearly and at the point of loss of synchronism, the maximum tractive effort is observed for the given constant speed. This procedure is tested with a number of speed values with a range of 0 to 4000 rpm and as a result, the figure 4.36 is plotted.

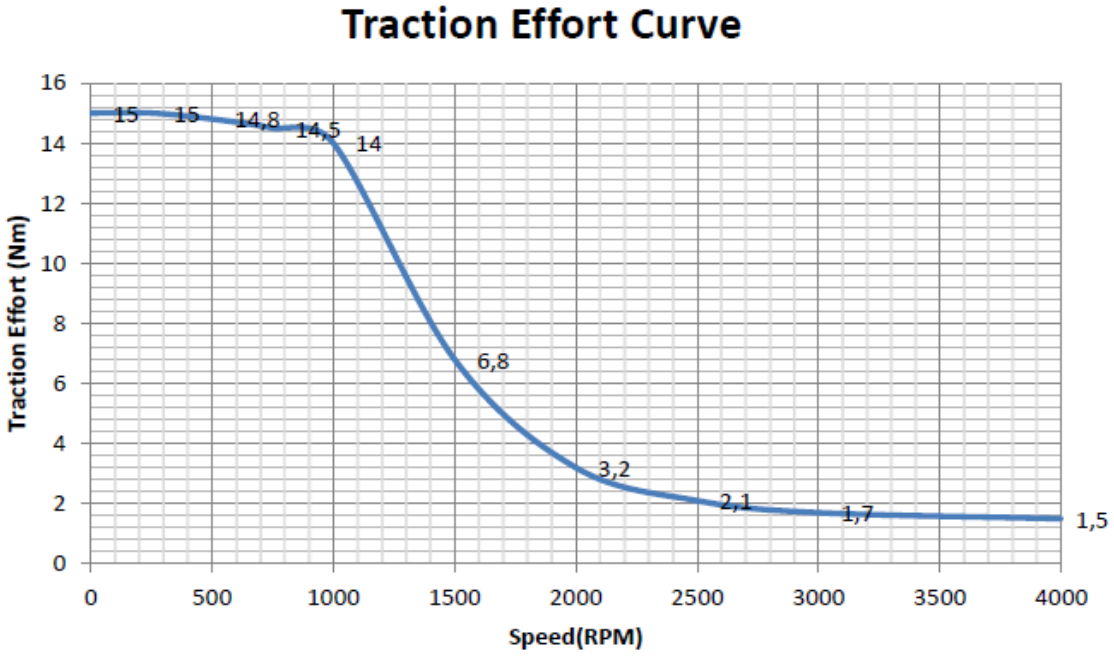

Figure 4.36: Traction Effort Curve of SynRM with Speed Controller

According to the graph, the maximum tractive effort of SynRM is 15 Nm. After the nominal speed, the curve is decreasing exponentially as described in concept in previous part.

Chapter 5

CONCLUSION AND FUTURE WORK

5.1 Conclusion

Todays industrial requirements make AC machines a necessity and therefore the number of studies regarding AC machines is increasing with each passing day. Until the beginning of 2000s, the most popular machine was the induction machine from the asynchronous machines family. However, developing drive technologies highlighted synchronous machines and nowadays, induction motors are gradually being phased out by PMSM and SynRM due to their higher efficiencies. Especially, the SynRM is gathering a lot of interest with its efficiency rates. Since the SynRM combines the benefits of induction motors such as robustness and PMSMs size, efficiency and synchronous speed, it deserves the attention of not only the researchers but also the industry. Moreover, due to its ferromagnetic rotor structure, which does not have any excitation winding or magnets on it, the production cost of SynRM is much lower than induction motors and PMSMs. SynRM also produces reluctance torque, enabling it to deliver a high power density. To improve produced reluctance torque several rotor types were constructed such as simple salient pole (SP) rotor, axially laminated anisotropy (ALA) rotor and transversally laminated asymmetric (TLA) rotor. Lately, researchers improved the efficiency of SynRM by inserting permanent magnets into the transversally laminated rotor structure. Although this technique increases the production cost of SynRM, it leads to improved power factor, increased saliency ratio and reduced torque ripples.

To model a SynRM, a mathematical model is derived from its equivalent circuit. To achieve this model, various key points in the SynRM design were inspected in Chapter 2 from a mathematical perspective. Since modeling any motor in three phase reference frame is so complex and time consuming, the SynRM is modeled in direct-quadrature-zero (d-q-0) reference frame. An equivalent circuit in d-q reference frame is allowed to derive equations for d-q axis voltage, current vectors and electromagnetic torque. Thanks to the d-q reference frame, SynRMs equations were also derived in the phasor domain. Because the low power factor is one of biggest disadvantages of SynRM, Chapter 2 particularly included the calculation of the power factor. As a result, an equation is derived to obtain a correlation between saliency ratio and maximum power factor.

In Chapter 3, two different types of control method are explained and their mathematical expressions are derived for a better understanding. Since the efficiency is of great importance for energy savings, minimizing the losses is one of the vital duties of control methods. In this regard, researchers revealed that the most effective ways to control SynRM are direct torque control and field oriented control methods because in these types of control methods, d-q current vectors can be controlled independently. When these current vectors are controlled independent from each other, an effective method of reducing the losses can be provided and efficiency can be enhanced substantially. By arranging the current vectors, an optimal operating point can be set for maximum efficiency and this point is called maximum torque per ampere point. This thesis investigates two types of control methods, which are called sensorless speed control and maximum torque per ampere control. In sensorless speed control, a voltage estimator block is constructed with the voltage equation at the optimal operating point and desired speed compared with the measured speed by PI controller. In the MTPA control, the control algorithm is constructed based on FOC method with PI-based current controller. For the desired torque, the MTPA point is calculated periodically by changing the d-q current vectors in order to reach maximum torque with the given current.

The simulations are done in MATLAB/Simulink. The Simulink block diagrams and results of the simulations are illustrated in Chapter 4. Firstly, SynRM is constructed with direct quadrature zero reference frame and sensorless speed controller is connected to the motor. d-q axis currents are limited at the stator in order to prevent damages which might be caused by high input current at the overloading cases. Moreover, the desired speed and

the desired torque are satisfied by the measured speed and torque, hence the precision of the model is validated. Then, from the MATLAB/Simulinks library, MTPA control for SynRM is equipped and modified to be compared with the first model. Lastly, Chapter 4 explains the traction effort curve and illustrates a plot for the simulated SynRM that shows the loadability of motor.

This study provided some background knowledge about the synchronous reluctance motors. Its working principle, rotor types and mathematical modelling are studied. A literature review over existing control strategies supplied information about field oriented control, maximum torque per ampere method and sensorless speed control. Not only electrical but also the mechanical behaviors of SynRM are simulated and investigated which fulfills the first objective of this thesis. Furthermore, the results which are obtained from simulations with both control types are compared and differences between them are evaluated. Ultimately, both objectives of this thesis have been satisfied.

5.2 Future Work

This study can be expanded by exploring the following:

- It would be interesting to perform the simulations with permanent magnet assisted synchronous reluctance motor(PMa-SynRM) which is the latest version of SynRM. Herewith, the effects of permanent magnets on the SynRM behaviors can be observed.
- Considering that the position of the rotor has already measured in both simulations, a position controller can be added to the both control methods.
- The experimental implementation of the methodology will be carried out with ABB's 1.5kW SynRM.

Chapter 6

REFERENCES

[1] R. Saidur, A review on electrical motors energy use and energy savings, Renewable and Sustainable Energy Reviews, vol. 14, no. 3, pp. 877898, Apr. 2010.

[2] A. Binder, Potentials for energy saving with modern drive technology a survey, in Proc. of IEEE International Symposium on Power Electronics, Electrical Drives, Automation and Motion, pp. 9095, 2008.

[3] B. Adkins, R. G. Harley, The General Theory of Alternating Current Machines: Application to Practical Problems New York: Wiley, ISBN 978-0-412-12080-0, pp. 2-10, 1975.

[4]S.L Herman, Electric Motor Control Clifton Park, New York: Delmar, ISBN-10: 1-4354-8575-4, pp.3-14, 2010.

[5]Carrier Corporation, Operation and Application of Variable Frequency Drive (VFD) Technology, Syracuse, New York : Carrier Corporation, pp.2-6, October 2005.

[6] A. von Jouanne, D. Rendusara, P. Enjeti, and W. Gray,"Filtering Techniques to Minimize the Effect of Long Motor Leads on PWM Inverter Fed AC Motor Drive Systems," IEEE Transactions on Industry Applications, 1996.

[7] H. Kiriyama, S.Kawano, Y.Honda, T.Higaki, S.Morimoto, Y.Takeda High Performance Synchronous Reluctance Motor with Multi-flux Barrier for the Appliance Indiustry, Osaka,Japan : IEEE Transactions on Industry Applications., 1998.

[8]ABB Catalog, Low voltage High output synchronous reluctance motors, April, 2016

[9]P.Matyska Advantages of Synchronous Reluctance Motors, Praha, Czech Republic, IEEE Transactions on Electrical Engineering, Vol. 3, No. 2, pp.44, 2014.

[10]J.M. Park, S.Kim, J.P. Hong, J.H. Lee Rotor Design on Torque Ripple Reduction for a Synchronous Reluctance Motor With Concentrated Winding Using Response Surface Methodology , IEEE Transactions on Magnetics, Vol. 42, No. 10, October, 2006.

[11]D.A. Staton, T.J.E. Miller, S.E. Wood, Maximizing the saliency ratio of the synchronous reluctance motor, Electric Power Applications, IEEE Proceedings B [see also IEE Proceedings-Electric Power Applications],Volume 140, Issue 4, Page(s):249 259, July 1993.

[12] T. A. Lipo, T. J. E. Miller, A. Vagati, I. Boldea, L. Malesani, and T. Fukao, Synchronous reluctance drives IEEE-IAS Annual Meeting, Denver, 1994.

[13] A. Vagati, The synchronous reluctance solution: a new alternative in A. C. drives", IEEE IECON, vol. 1, pp.1-13, 1994.

[14] I. Boldea (2017) , Linear Electric Machines, Drives, and MAGLEVs Handbook, CRC Press, ISBN 9781138076334.

[15] P. L. Alger, The Nature of Polyphase Induction Machines, New York: Wiley, 1951

[16] R. V. Hamid, A. Toliyat, B. Akin, R. Poley, "Power Factor Improvement of Synchronous Reluctance Motors (SynRM) Using Permanent Magnets for Drive Size Reduction", Twenty-Seventh Annual IEEE Applied Power Electronics Conference and Exposition (APEC), IEEE,Feb. 2012

[17] R.D. Lorenz, D.B. Lawson, A simplified approach to continuous on-line tuning of field oriented induction machine drives, IEEE Transactions on Industry Application, vol. 26, no. 3, pp. 420-425, May/June 1990.

[18] Agamloh E.B. (2009). A Comparison of Direct and Indirect Measurement of Induction Motor Efficiency, IEEE Electric Machines and Drives Conf. pp. 36-42.

[19] Lipo, T. A., Synchronous reluctance machines a viable alternative for AC drives. Wisconsin Electric Machines and Power Electronics Consortium, Research report, 1991.

[20] Boglietti A., Abruzzi C.D. (2008), Induction and Synchronous Reluctance Motor Comparison, IEEE Transactions on Industry Application, vol. 34, pp. 2041-2044.

[21] Bolognani S., Peretti L., Zigliotto M. (2011), Online MTPA Control Strategy for DTC Synchronous-Reluctance-Motor Drives, IEEE Transactions on Industry Application, vol. 26, no.1, pp. 20-28.

[22] Jansen, P.L., and Lorenz, R.D. (1995), Transducerless position and velocity estimation in induction and salient A.C machines, IEEE Transactions on Industry Applications, Vol. 31, no. 2, pp. 240247.

[23] Fellani M.A., Abaid D.E. (2010) Matlab/Simulink-Based Transient Stability Analysis Of A Sensorless Synchronous Reluctance Motor, World Academy of Science, Engineering and Technology International Journal of Electrical and Computer Engineering Vol:4, No:8, pp. 1364-1368.

[24] Y. Inoue, S. Morimoto, and M. Sanada, (2011) A Novel Control Scheme for Maximum Power Operation of Synchronous Reluctance Motors Including Maximum Torque Per Flux Control, IEEE Trans. Ind. Appl., vol. 47, no. 1, pp.115121.

[25] Ferdous S.M., Garcia P., Oninda M. A. M., Hoque . (2016), MTPA and Field Weakening Control of Synchronous Reluctance Motor, IEEE Transactions on Industry Applications, Vol.16, no. 9, pp. 598-601.

[26] P. Niazi (2005), Permanent Magnet Assisted Synchronous Reluctance Motor Design and Performance Improvement, Doctoral Dissertation. Texas AM University, Texas, USA.

[27] D. K. Singh, E. S. Thakur, S. Kesharwani, Dr. A.S.Zadgaonkar ," Analysis Of Generated Harmonics Due To Single Phase PWM AC Drives Load On Power System Using Artificial Neural Network" ,International Journal of Advanced Research in Engineering and Technology (IJARET),Volume 5, Issue 2, February (2014), pp. 173-185.

[28] R.R. Moghaddam (2007), "Synchronous Reluctance Machine (SynRM) Design", Master Thesis, Royal Institute of Technology, Stockholm

[29] M. A. Hannan, J. A. Ali, A. Mohamed, A. Hussai, "Optimization techniques to enhance the performance of induction motor drives: A review" , Renewable and Sustainable Energy Reviews, June 2017.

[30] V. Jaikrishna (2013), "Principle Of Operation Of Synchronous Reluctance Motor and Mathematical Model ", www.technologyfuturae.com.

[31] W.B. Lin, H.K. Chiang (2013), "Super-Twisting Algorithm Second-Order Sliding Mode Control for a Synchronous Reluctance Motor Speed Drive", Mathematical Problems in Engineering, Volume 2013, Article ID 632061,

[32] D. Vimalakeerthy, Dr.M.Y.Sanavullah,"Development Of New Design To Improve The Performance Of Permanent Magnet Synchronous Reluctance Motor Using Finite Element Method",International Journal of Engineering Science and Technology (IJEST), Vol. 3, No. 2, Feb 2011

[33] S.M.Ferdous, P. Garcia, M. A. M. Oninda, Md. A. Hoque, "MTPA and Field Weakening Control of Synchronous Reluctance Motor", 9th International Conference on Electrical and Computer Engineering, December 2016, Dhaka, Bangladesh

Appendix A

APPENDIX

A.1 Parameters of SynRM

The simulated SynRM's parameters are illustrated below.

Parameters	Values	Unit
R_s	4,195	Ohms
L_d	0,1796	H
L_q	0,0699	H
L_{ls}	0,389	H
J	0,0067	$Kg.m^2$
P	2	number
V_{dc}	400	V
D_f	0,007	Nm.sec/rad

Figure A.1: Parameters of SynRM